JOURNAL OF THE SOUTH AFRICAN CHEMICAL INSTITUTE

NEW
SERIES
VOLUME VIII
NUMBER .. 2

September
1955
September

NUWE
SERIE
DEEL VIII
NOMMER .. 2

Published by the Institute, Kelvin House, Johannesburg

Uitgegee deur die Instituut, Kelvinhuis, Johannesburg

Price / *Prys* } 7/6

JOERNAAL VAN DIE SUID-AFRIKAANSE CHEMIESE INSTITUUT

ethyl acetate

B.S.S. 533/1934

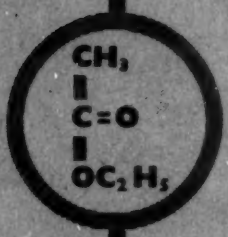

SPECIFICATIONS:

SPECIFIC GRAVITY 15.5°/15.5°C : 0.906-0.908.
20°/20°C : 0.901-0.904.
DISTILLATION RANGE : 95% between 76°-79°C.
ACIDITY (As acetic acid): Max. 0.01%
ESTER CONTENT : Min. 98%
MOISTURE : Free.
RESIDUE : Max. 0.01%

USES:

As a solvent for nitrocellulose, celluloid, gums and resins in the manufacture of lacquers of all types, leather cloth, and dopes.
As a solvent for aniline, other colours, and synthetic resins in the manufacture of quick-drying printing inks.
In acetic acid recovery.
As a constituent of synthetic flavouring essences.

N.C.P.

Head Office
GERMISTON, TRANSVAAL

NATIONAL CHEMICAL PRODUCTS LIMITED

Industrial Fermentation Specialists and producers of organic solvents

Subsidiary Company: UMGENI DISTILLERIES LTD., SEA COW LAKE RD., BOX 2204, DURBAN.
Cape Town Office: National Chemical Products Ltd., 532 Grand Parade Centre, Adderley Street, Box 3430, Cape Town.
Port Elizabeth Office: National Chemical Products Ltd., 102 Martien House, Strand Street, Box 1452, Port Elizabeth.
Salisbury Office: National Chemical Products Ltd., Dolphin House, Moffatt Street, Salisbury.
Agents: Poly-Resin Products Ltd., East London; Universal Agencies, Bloemfontein; Leslie & Anderson (East Africa) Limited, Mombasa.

Die Redakteur en die Suid-Afrikaanse Chemiese Instituut aanvaar geen verantwoordelikheid vir verklarings wat gemaak word of menings wat uitgespreek word deur bydraers nie.

The Editor and the South African Chemical Institute assume no responsibility for statements made and opinions expressed by contributors.

CONTENTS — INHOUD

A PHYSICO-CHEMICAL STUDY OF THE PROTEINS FROM THE OYSTER NUT (*TELFAIREA PEDATA*)

by

F. J. JOUBERT

OPSOMMING

'n Fisies-chemiese studie van die eiwitte van die oyster-neut (*Telfairea pedata*) is onderneem. In die ultrasentrifuge het die eiwitte van die oyster-neut een hoof-komponent en klein konsentrasies van ander komponente getoon. Die hoof-komponent is van die ander komponente deur ammoniumsulfaatfraksionasie gesuiwer. Deur gebruik te maak van sedimentasie- en diffusieopmetings is 'n molekulêrgewig van 311,000 vir die hoof-komponent gevind.

SUMMARY

A physico-chemical study has been made of the proteins of the oyster nut (*Telfairea pedata*). In the ultracentrifuge the proteins from the oyster nut showed one major component and small concentrations of other components. The major component was separated from the minor components by ammonium sulphate fractionation. Using sedimentation and diffusion measurements a molecular weight of 311,000 was found for the major component.

The oyster nut is produced on a vine of the family Cucurbitaceae indigenous to East Africa. The nuts and their possible uses are fully described by Poppleton[1]. The oyster nut kernels contain 64 *per cent.* of a non-drying oil and the defatted meal is 78 *per cent.* protein. The present communication is concerned with the examination of the proteins of the oyster nut by ultracentrifuge methods.

METHODS

Sedimentation studies were carried out in a Spinco electrically driven ultracentrifuge manufactured by Messrs. Specialised Instrument Corporation, Belmont, California. All the runs were performed at *ca.* 60,000 r.p.m. equivalent to a centrifugal force of *ca.* 250,000 g.

Diffusion coefficients have been determined at 20°C by the free boundary method using the Tiselius U-tube for boundary formation. A plunger type of compensator was used to move the boundary between protein and buffer solution into the observation channels without disturbances.

PREPARATION OF THE PROTEINS

Dehulled oyster nuts were defatted by repeated extraction with hexane by using a Waring blendor. The proteins of the oil-free oyster nut meal were completely extracted with three separate volumes of 10 *per cent.* aqueous sodium chloride solution over a period of 24 hours at room temperature. The final protein extract was centrifuged clear at 2,500 r.p.m. The extracted proteins were precipitated by adding ammonium sulphate to 85 *per cent.* saturation. The protein obtained was soluble only in buffers of relatively high salt concentration. This preparation, when examined in the ultracentrifuge in borate buffer of ionic strength (I) = 0·3 and pH = 8·8, revealed (Fig. 1 (a)) one major component of sedimentation constant of 12·5 Svedberg Units (S.U.) and small quantities of components of 19·4, 7·8 and 1·6 S.U. (respectively designated as the $S_{12\cdot5}$, $S_{19\cdot4}$, $S_{7\cdot8}$ and $S_{1\cdot6}$ components).

The minor components were fractionated from the major $S_{12\cdot5}$ component as outlined in Fig. 2.

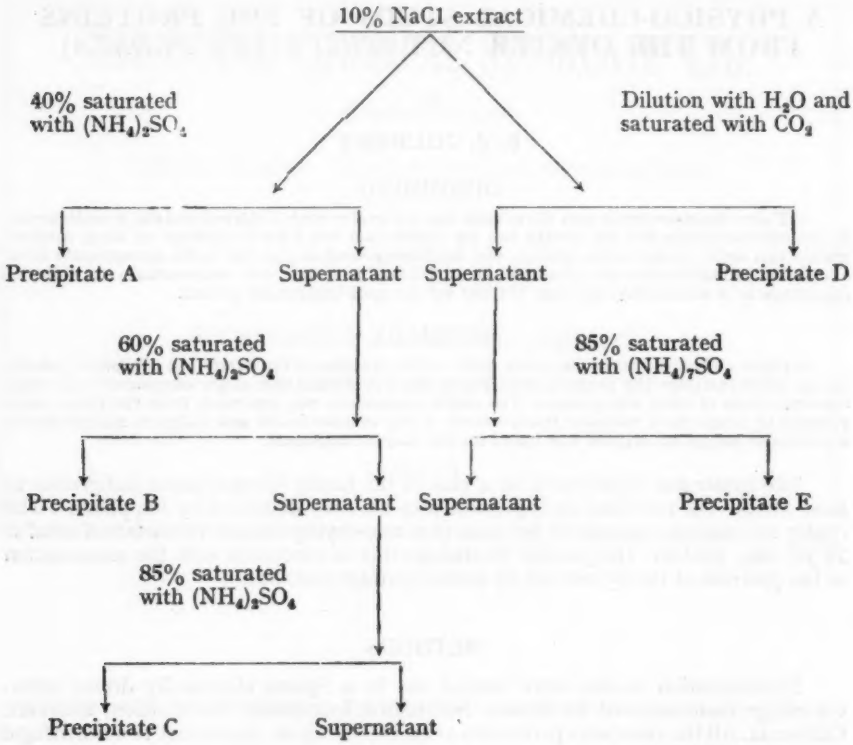

Fig. 2.
Scheme for the fractionation of oyster nut proteins.

When the 10 *per cent.* sodium chloride protein extract was saturated to 40 *per cent.* with ammonium sulphate, about 70 *per cent.* of the proteins were precipitated (Precipitate A). On the addition of ammonium sulphate to 60 *per cent.* saturation a further 20 *per cent.* of the proteins were precipitated (Precipitate B) and at 85 *per cent.* the residual proteins (Precipitate C). In the second preparation 90 *per cent.* of the proteins extracted with 10 *per cent.* sodium chloride were precipitated by adding six volumes of water at 4°C to each volume of the extract followed by saturation with carbon dioxide (Precipitate D). When the supernatant of Precipitate D was saturated to 85 *per cent.* saturation with ammonium sulphate, the residual proteins were precipitated (Precipitate E).

Fig. 1 gives sedimentation diagrams in borate buffer of I = 0·3, pH = 8·8 of the different precipitates outlined in Fig. 2 and the sedimentation constants are shown in Table I. Whereas a major $S_{12\cdot5}$ component almost free from the minor components was obtained for Precipitate A, Precipitate D still contained some of the $S_{7\cdot8}$ component. For Precipitate B major $S_{12\cdot5}$, $S_{7\cdot8}$ and $S_{1\cdot6}$ components were found. Precipitates C and E, however, contained almost pure $S_{1\cdot6}$ component. By using the described methods, it was thus possible to get pure fractions of the $S_{12\cdot5}$ and $S_{1\cdot6}$ components.

Precipitate A was also examined in phosphate buffer of I = 0·3, pH = 7·0 and borate buffer of I = 0·1, pH = 9·0. The sedimentation diagrams obtained are given in Fig. 1 (g) and (h) respectively, and sedimentation constants in Table I. As shown, no change in sedimentation diagrams and sedimentation constants was found. It wouldt hus appear that the $S_{12\cdot5}$ component was stable with respect to these changes in salt concentration and pH.

MOLECULAR WEIGHT OF THE $S_{12\cdot5}$ COMPONENT

Table I also contains sedimentation constants of Precipitate A at different concentrations. A slight increase in the sedimentation constant with decreasing concentration is observed. When the results of Table I were extrapolated to zero concentration, a value of 13·3 S.U. was found for the sedimentation constant.

In Table II the diffusion coefficients determined in borate buffer of I = 0·3, pH = 8·8 at 20°C, calculated by the maximum height, D°_{20} (H_m) and the standard deviation, D°_{20} (σ^2) methods, for Precipitate A are listed. The two methods of calculation gave approximately the same diffusion coefficient for Precipitate A, indicating a high degree of homogeneity[2] in accordance with the ultracentrifugal observations.

Using the diffusion data of Table II and the value of the sedimentation constant at zero concentration, the molecular weight and frictional ratio of Table III were found. The molecular weight obtained is comparable with values reported for other seed globulins.[3]

TABLE I

Sedimentation constants of oyster nut proteins in borate buffer, I = 0·3, pH = 8·8.

Fraction		Concentration *per cent.*	Sedimentation constants (S°_{20}–values)
Total		1·2	19·4, 12·5, 7·8, 1·6
Precipitate	A	1·3	–, 12·5, –, –
,,	B	1·0	–, 12·9, 7·9, 1·7
,,	C	0·5	–, –, –, 1·7
,,	D	0·9	19·3, 12·9, 7·9, –
,,	E	0·6	–, –, –, 1·6
,,	A	1·30	–, 12·5, –, –
,,	A	0·98	–, 12·8, –, –
,,	A	0·65	–, 12·9, –, –
,,	A	0·33	–, 13·1, –, –
,,	A[1]	1·0	–, 12·8, –, –
,,	A[2]	0·5	–, 13·2, –, –

[1] Sedimentation in phosphate buffer, I = 0·3, pH = 7·0.
[2] Sedimentation in borate buffer, I = 0·1, pH = 9·0.

TABLE II

Diffusion coefficient of Precipitate A in borate buffer, I = 0·3, pH = 8·8.

Time in hours	D°_{20} (H_m) $\times 10^{-7}$ cm.^{2}/sec.	D°_{20} (σ^2) $\times 10^{-7}$ cm.^{2}/sec.
9·35	—	3·93
21·38	3·96	4·08
25·78	3·96	4·06
30·30	3·92	3·93
35·97	3·94	4·04
45·65	4·01	4·09
Average	3·96	4·02

TABLE III

Molecular weight of the $S_{12\cdot5}$ component.

D°_{20} cm.^{2} sec.$^{-1}$	$3·99 \times 10^{-7}$
S°_{20} Svedberg Units	13·3
Partial specific volume (assumed)	0·74
Molecular weight	311,000
Frictional ratio	1·19

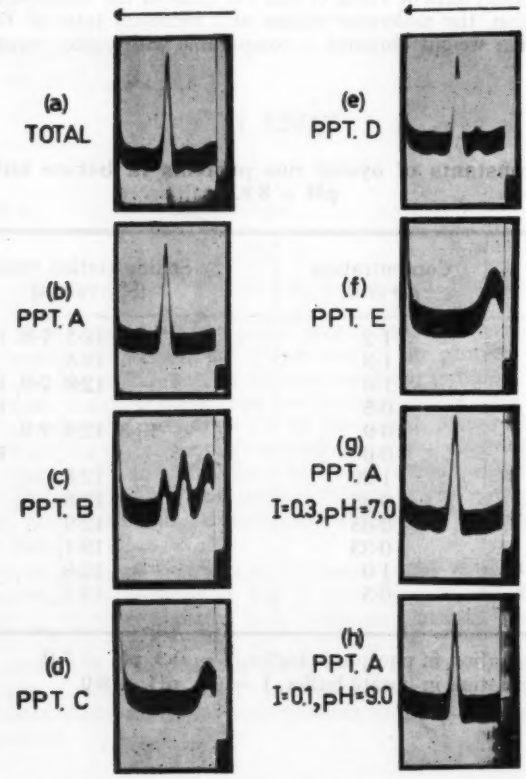

Fig. 1. Sedimentation diagrams of oyster nut proteins.

This paper is published by permission of the South African Council for Scientific and Industrial Research.

National Chemical Research Laboratory,
South African Council for Scientific and Industrial Research,
Pretoria, South Africa. *Received March* 14, 1955.

REFERENCES

[1] Poppleton, W. J., *East African Agric. J.*, 1939, **5**, 114.
[2] Charlwood, P. A., *J. Phys. Chem.*, 1953, **57**, 125.
[3] Weissberger, A., "Physical Methods of Organic Chemistry," Vol. I, Part I, Interscience Publishers, 1949, 706.

CHEMISTRY OF NARAS SEED (*ACANTHOSICYOS HORRIDA*, HOOK)

PART II—A PHYSICO-CHEMICAL STUDY OF NARAS SEED PROTEINS IN SODIUM DODECYL SULPHATE SOLUTIONS

by

F. J. JOUBERT

OPSOMMING

'n Fisies-chemiese studie van die eiwitte bevat in narassaad is in natriumdodesielsulfaat-oplossings onderneem. Die molekulêrgewig van die kompleks wat gevorm word hang af van die kondisies waaronder dit berei was, maar is altyd baie kleiner as die van die oorspronklike eiwit. Deur gebruik te maak van verskillende metodes is 'n gemiddelde molekulêrgewig van 84,000 gevind vir 'n kompleks berei by 'n ioniese sterkte (I) van 0·1 en pH = 7·8. 'n Hoër molekulêrgewig is gevind vir komplekse berei by I = 0·2, pH = 7·8. Die komplekse ondergaan 'n omkeerbare assosiasie-dissosiase reaksie wanneer die pH en ioniese sterkte verander word.

SUMMARY

A physico-chemical study has been made of the proteins of naras seed dissolved in sodium dodecyl sulphate solutions. The molecular weight of the complex which formed depended on the conditions of preparation but was always very much lower than that of the original protein. For complexes prepared at an ionic strength (I) of 0·1 and pH = 7·8, an average molecular weight of 84,000 was found by different methods. A higher molecular weight was found for complexes prepared at I = 0·2, pH = 7·8. The complexes underwent a reversible association-dissociation reaction when pH and ionic strength were varied.

Since the early work of Bull and Neurath[1] on the effect of sodium dodecyl sulphate on egg albumin, a considerable body of work on the action of long chain detergents on the simpler protein molecules has been published. Little has been done along this line on the seed globulins. The interaction of paraffin chain sulphates of differing chain length with the seed globulin, arachin, has been studied by Johnson and Joubert[2]. At low sulphate concentrations these writers found that association of arachin half-molecules is promoted. At higher detergent concentrations a new slowly-sedimenting component was observed in the ultracentrifuge and more rapid components in electrophoresis.

Naras seed protein was practically insoluble in buffers of low ionic strength (e.g. phosphate buffer of I = 0·1, pH = 7·8). It was, however, observed that the protein dissolved readily in these buffers in the presence of sodium dodecyl sulphate (S.D.S.). This fact alone seems to indicate that a protein-detergent complex has been formed.

Whereas in Part I[3] the physico-chemical properties of naras seed protein in ordinary buffers were described, the present work reports an examination of the complexes which formed when naras seed protein was dissolved in buffer containing S.D.S.

METHODS

A Brice-Phoenix light scattering photometer[4] was used for the measurement of the light scattered at 45°, 90° and 135° to the incident beam. The blue mercury line of wavelength 4358 Å and the green 5461 Å were used for turbidity measurements. The solutions were prepared dust free by centrifugation at *ca.* 20,000 r.p.m. for 30 minutes and a final ultrafiltration through nitrocellulose membranes as described by Goring and Johnson[5]. Benzene, a standard sample of polystryene and Ludox

solutions were used for absolute calibration of light scattering intensities at 90° as described[6].

Electrophoresis was carried out in a Tiselius electrophoretic apparatus manufactured by Messrs. Hilger Watts Ltd., using a medium U-tube equipped with a long centre section. Electrophoresis was carried out at 20°C. with appropriately limited field strengths[7]. Dialysis of solutions was routinely performed in a slowly rotating cellophane bag against a large volume of the required buffer solution.

Sedimentation studies were carried out in a Spinco electrically driven ultracentrifuge manufactured by Messrs. Specialised Instrument Corporation, Belmont, California. All the runs were performed at *ca.* 60,000 r.p.m., equivalent to a centrifugal force of *ca.* 250,000 *g*.

Diffusion coefficients have been determined at 20°C. by the free boundary method using the Tiselius U-tube for boundary formation. A plunger type of compensator was used to move the boundary between protein and buffer solution into the observation channel without disturbances.

Osmotic pressures were measured in an Adair[8] type of osmometer, and were corrected for capillary rise observed in the same osmometer with the same solutions.

Relative viscosities were measured using a Cannon-Fenske viscometer in a water bath thermostatically controlled to $20 \pm 0{\cdot}02$°C.

Refractive index increments were measured at 5780 Å using a modified Pulfrich refractometer with a divided cell and values at 4358 Å and 5461 Å were calculated by using Perlmann and Longsworth's[9] equation.

MATERIALS

Naras seed protein was prepared as described by Joubert and Cooper[3]. The proteins of oil-free naras seed meal were extracted with 10 *per cent.* sodium chloride and then four volumes of water were added to each volume of the extract, causing precipitation of the extracted protein. The precipitate, washed free from chloride with cold water, was freeze-dried.

Purified S.D.S. was kindly provided by Messrs. Imperial Chemical Industries, Ltd. When examined electrophoretically at 20°C, the S.D.S. migrated with a single boundary.

Protein-detergent complexes were prepared as follows: 1 *per cent.* Naras seed protein was added to phosphate buffer, $I = 0{\cdot}1$, $pH = 7{\cdot}8$ containing 1 *per cent.* S.D.S. at room temperature and the protein was completely dissolved in about one hour. The detergent-protein solution was cooled to 4°C and a crystalline precipitate formed. This was filtered off in the cold and dissolved in buffer at room temperature. It gave a negative test for protein and was identified as pure S.D.S., so that excess S.D.S. was removed to a large extent as a result of its limited solubility in the cold (*ca.* 0·05 *per cent.* at 1°C). The detergent-protein solution was next dialysed against a large volume buffer of $I = 0{\cdot}1$, $pH = 7{\cdot}8$, containing a small amount (0·02 *per cent.*) S.D.S. This extra amount of detergent was added to the buffer to repress the dissociation of the complex, as it was observed that prolonged dialysis of the complex solution against buffer containing no detergent caused precipitation of the complex.

RESULTS

The composition of the complex was estimated by determining (i) dry weight concentration and (ii) kjeldahl concentration on the same dialysed complex solution. The dry weight gave the complex concentration and the kjeldahl concentration, using a nitrogen content of 18·12 *per cent.* for the protein, the weight of protein

associated with the complex and hence the amount of S.D.S. combined with protein was obtained. In so doing it was assumed that in dialysis of complex solutions free S.D.S. was equally distributed between complex solution and buffer, and that the difference between their concentrations gave an estimate of the complex concentration. The composition of complexes determined in this way is shown in Tables I and II. As shown, the average detergent uptakes at I = 0·1 and I = 0·2, pH 7·8 were the same.

Table III contains refractive index values of complexes prepared under different conditions. The refractive index values of the complexes were lower than those found for the protein, but in agreement with the detergent uptake the same values were found at I = 0·1 and I = 0·2, pH = 7·8.

TABLE I

Composition of complex prepared at I = 0·1 and pH = 7·8

Protein concentration by kjeldahl (*g./100 c.c.*)	*Complex concentration dry weight* (*g./100 c.c.*)	*g. S.D.S./g. protein in complex*
0·433	0·609	0·41
0·681	1·044	0·53
0·776	1·145	0·48
0·840	1·246	0·48
0·874	1·246	0·43
1·059	1·584	0·49
1·117	1·645	0·45
		Average 0·47

TABLE II

Composition of complex prepared at I = 0·2 and pH = 7·8

Protein concentration by kjeldahl (*g./100 c.c.*)	*Complex conentration dry weight* (*g./100 c.c.*)	*g. S.D.S./g. protein in complex*
0·658	0·949	0·44
0·909	1·397	0·54
0·980	1·421	0·45
1·018	1·521	0·49
1·057	1·564	0·48
		Average 0·47

TABLE III

Refractive index increment values of complexes.

Preparation	5780 Å	5461 Å	4358 Å
Original protein	0·187	0·188	0·196
Complex prepared at I=0·1, pH=7·8	0·164	0·165	0·171
Complex prepared at I=0·2, pH=7·8	0·164	0·165	0·171

In Table IV the light scattering molecular weights found for complexes prepared at different conditions of pH values and ionic strengths are given and a typical graph of $\frac{c}{\tau}$ against c is shown in Fig. 1.

In all cases the molecular weight of the complexes was very much lower than that of the original protein, hence the protein was significanctly broken down in complex formation.

TABLE IV

Light scattering molecular weights of complexes.

Preparation		*Molecular weight*		
I	pH	4358 Å	5461 Å	Average
Original protein		370,000	388,000	379,000
0·1	6·6	122,000	141,000	132,000
0·1	7·8	83,000	93,400	88,200
0·1	9·0	98,700	107,000	102,900
0·2	7·8	161,000 153,000	169,000 165,000	162,000

Complexes prepared as in Table IV were examined in the ultracentrifuge (Fig. 2). At I = 0·1, pH = 6·6, 7·8 and 9·0 single sedimenting components were observed, but at I = 0·2 and 0·4, pH = 7·8 small concentrations of an additional fast sedimenting component were noticed. Sedimentation constants of the complexes are given in Table V.

TABLE V

Sedimentation constants of complexes at a concentration of 1·54 *per cent.*

Preparation		S°_{20}–*values*
I	pH	
Original protein		12·6
0·1	6·6	2·87
0·1	7·8	2·64
0·1	9·0	2·88
0·2	7·8	3·29 3·29 3·36 } 3·31
0·4	7·8	3·98

Here again sedimentation constants of the complexes were very much lower than that of the original protein.

Fig. 3 shows electrophoretic diagrams of complexes prepared at different conditions of pH and ionic strength. Although single boundaries on both ascending and descending sides were obtained, it was felt that the spreading of some of the electrophoresis peaks must be attributed to some degree of electrophoretic heterogeneity. The mobility of the globulin itself could not be measured, owing to its poor solubility in solutions of moderate ionic strength, but it probably compares with mobilities

of other seed globulins, e.g., arachin[10], studied under similar conditions. The mobilities of the complexes in Table VI are about double the mobility to be expected of the globulin, and so probably indicate that the net negative charge on the protein was considerably increased by complex formation.

TABLE VI

Electrophoretic mobilities of complexes at 20°C.

Preparation		*Mobility* $\times 10^{-4}$ *cm.*^{2} *sec.*$^{-1}$ *volt*$^{-1}$	
I	*pH*	*Ascending*	*Descending*
0·1	6·6	−2·31	−2·03
0·1	7·8	−2·52	−2·28
0·1	9·0	−2·27	−1·88
0·2	7·8	−2·03	−1·79

It will be noted that the light scattering molecular weights as well as the sedimentation constants were not constant in various buffer solutions. In order to throw more light on this, the two extremes in Table IV were examined in some detail. These were both at the same pH (7·8), but at different ionic strengths, I = 0·1 and I = 0·2. In Table VII diffusion coefficients determined at 20°C for these two preparations are summarised. It will be seen that the coefficient for I = 0·1 was higher than for I = 0·2, in accord with a lower molecular weight. More important, the values calculated by the maximum height D°_{20} (H_m) and standard deviation, D°_{20} (σ^2) methods were in agreement in each case. This suggests that molecular weights in each solution were reasonably homogeneous.

TABLE VII

Diffusion coefficients of complexes.

Preparation	D°_{20} (H_m) $\times 10^{-7}$ *cm.*^{2}*/sec.*	D°_{20} (σ^2) $\times 10^{-7}$ *cm.*^{2}*/sec.*
I = 0·1, pH = 7·8	5·42	5·51
	5·38	5·50
	5·80	5·77
	5·63	5·69
	Average 5·56	5·62
I = 0·2, pH = 7·8	4·26	4·32
	4·24	4·36
	4·58	4·55
	4·53	4·57
	Average 4·40	4·45

In Fig. 4 the corrected sedimentation constants (S°_{20}—values) for complexes prepared at I = 0·1, 0·2 and pH = 7·8 are plotted against concentration. As shown sedimentation constants increased with decreasing concentration. Molecular weights and frictional ratios of Table VIII were calculated using the values of sedimentation constants at zero concentration of Fig. 5, the diffusion data of Table VII and assuming a partial specific volume of 0·78 for complexes. This value was calculated on the

assumption that the partial specific volume of the complex is an additive function of those of its components.

TABLE VIII

Sedimentation molecular weight of complexes.

Preparation	$I = 0{\cdot}1$, $pH = 7{\cdot}8$	$I = 0{\cdot}2$, $pH = 7{\cdot}8$
D°_{20}cm.^{2} sec.$^{-1}$	$5{\cdot}62 \times 10^{-7}$	$4{\cdot}45 \times 10^{-7}$
S°_{20} Svedberg units	4·02	4·78
Partial specific volume	0·78	0·78
Molecular weight	79,000	118,000
Frictional ratio	1·31	1·44

The molecular weights of the complexes were also determined by osmotic pressure measurements (Table IX).

TABLE IX

Osmotic pressure of complexes.

Preparation	*c (concentration g./100 c.c.)*	*π (osmotic pressure cm. H_2O)*	*π/c*
I = 0·2, pH = 7·8	1·900	4·40	2·32
	1·457	3·03	2·08
	0·960	2·15	2·24
	0·569	1·18	2·07
I = 0·1, pH = 7·8	1·325	4·57	3·45
	0·960	3·08	3·21
	0·664	2·07	3·12
	0·373	1·15	3·08

When the results of Table IX are extrapolated to zero concentration, values of 3·00 and 1·95 were respectively found for π/c for complexes prepared at I = 0·1, 0·2 and pH = 7·8. These values correspond to number average molecular weights of 80,000 at I = 0·1, pH = 7·8 and 123,000 at I = 0·2, pH = 7·8.

In Fig. 5 the viscosity increments $\left(\frac{\eta sp}{c}\right)$ for complexes prepared at I = 0·1, 0·2 and pH = 7·8 are plotted against concentration. From the intrinsic viscosity $\left(\frac{\eta sp}{c}\right)_{c \to o}$ values using Polson's[11] equation and assuming a partial specific volume of 0·78 for the complexes axial ratios $\left(\frac{b}{a}\right)$ were calculated. By substitution of these values into Perrin's[12] formula, frictional ratios $\left(\frac{f}{f_0}\right)$ were obtained. Together with the diffusion coefficients, D°_{20} (σ^2), these give the molecular weights of Table X.

TABLE X

Viscosity results of complexes.

Preparation	$\left(\frac{\eta sp}{c}\right)_{c \to o}$	$\left(\frac{b}{a}\right)$	$\left(\frac{f}{f_0}\right)$	$D^{\circ}_{20} \times 10^{-7}$ cm.²/sec.	mol. weight
I=0·1, pH=7·8	4·9	4·8	1·25	5·62	89,000
I=0·2, pH=7·8	5·4	5·5	1·29	4·45	163,000

In Table XI the molecular weights found by the different methods are sumarised.

TABLE XI

Molecular weights of complexes.

Preparation	*Molecular weights*	
	I = 0·1, pH = 7·8	I = 0·2, pH = 7·8
Sedimentation and diffusion ..	79,000	118,000
Osmotic pressure	80,000	123,000
Light scattering	88,200	162,000
Viscosity and diffusion ..	89,000	163,000

Molecular weights calculated by the different methods showed reasonable agreement for complexes prepared at I = 0·1, pH = 7·8, but were very much different for complexes prepared at I = 0·2, pH = 7·8. Although diffusion measurements indicated that complexes prepared at I = 0·2, pH = 7·8 were reasonable homogeneous, the difference between the light scattering (weight average) and osmotic pressure (number average) molecular weights indicates some degree of heterogeneity. Signs of a heavier component are noticed in the sedimentation diagrams (Fig. 2) of complexes prepared at I = 0·2. Thus will give rise to increased light scattering and viscosity molecular weights. The molecular weight obtained from sedimentation and diffusion measurements is rather low, but as the extrapolation of the sedimentation data of Fig. 4 is uncertain this is not surprising.

It would appear that, at pH = 7·8 dissociation takes place when the ionic strength is decreased from 0·2 to 0·1. Some further experiments were carried out to test this point. A naras seed protein-S.D.S. complex was prepared at I = 0·2, pH = 7·8 (light scattering molecular weight = 162,000 and $S^{\circ}_{20} = 3{\cdot}29$), and this protein-S.D.S. solution was then dialysed for 24 hours against buffer I = 0·1, pH = 7·8. For the resulting solution a single peak ($S^{\circ}_{20} = 3{\cdot}01$) was found in the ultracentrifuge and a light scattering molecular weight of 120,000 was obtained. Similarly a complex was prepared at I = 0·1, pH = 7·8 (light scattering molecular weight = 88,200 and $S^{\circ}_{20} = 2{\cdot}64$) and, when this complex was dialysed for 24 hours against buffer I = 0·2, pH = 7·8, a single peak ($S^{\circ}_{20} = 3{\cdot}16$) was obtained in the ultracentrifuge and a light scattering molecular weight of 130,000 was found. These experiments suggest a slow dissociation when ionic strength is decreased and a slow association when ionic strength is increased. As shown in Table I and II the composition of the complex is the same in both solutions, so that dissociation is due to splitting of the protein molecule rather than to loss of detergent.

On the above basis it would follow that the molecular weights in Table IV at I = 0·1, and pH values other than 7·8 arise from variable proportion of dissociated

and undissociated molecules. Because one peak only was always observed in the ultracentrifuge at conditions where at least a mixture of dissociated and undissociated molecules was expected, it would appear that dissociated and undissociated molecules could not be resolved by the ultracentrifuge.

Whereas it was possible to dissolve naras seed proteins in buffers of low ionic strength with the aid of S.D.S., the low molecular weight of the resulting complexes, compared with that of the original protein, indicates that considerable disaggregation and probably severe structural changes of the protein have occurred. The addition of S.D.S. to arachin in solution[2] causes a similar breakdown of a high molecular weight protein.

As described earlier, protein-S.D.S. complexes appeared to undergo a reversible association-dissociation reaction when pH and ionic strength were varied, but without alteration of the composition of the complexes. This composition (0·47 g. S.D.S./g. protein) corresponds to the binding of 615 detergent molecules per protein molecule of molecular weight 377,000. The amino acid composition of naras seed protein is not yet available, but it would appear that for seed globulins of similar molecular weight the total number of positively charged groups per molecule is of the order of 300 to 400 (e.g., 382 for edestin[1,3] and 332 for arachin[2]). If a similar number is assumed for naras seed globulin, it follows that the number of detergent molecules bound per gram of naras seed protein exceeds its number of positively charged groups. This may be compared to arachin[2], in which the proportion of detergent groups was even larger, about 1 g. S.D.S./g. protein.

Using molecular weights of 84,000 and 160,000 respectively for complexes prepared at I = 0·1, 0·2 and pH = 7·8, calculations from the known composition of the complexes have shown that complexes have been formed in which the weight of protein per molecule of complex is about 60,000 and 120,000 for preparations at I = 0·1 and I = 0·2, pH = 7·8 respectively. This suggests breakdown of the original protein molecule into sixths at I = 0·1 and thirds at I = 0·2.

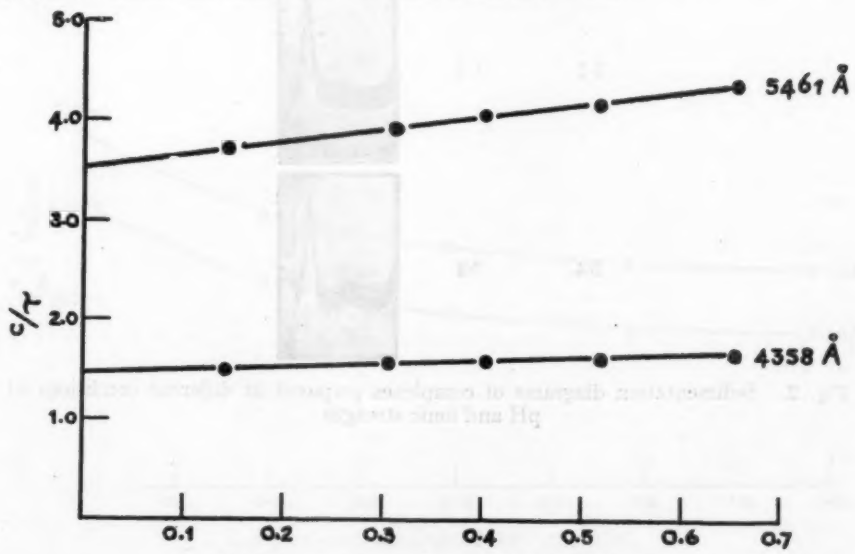

Fig. 1. c/τ against C for complex prepared at I = 0·1, pH = 7·8.

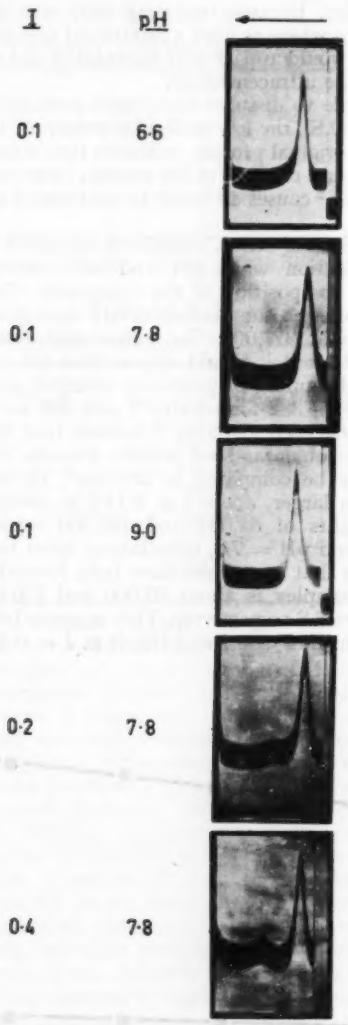

Fig. 2. Sedimentation diagrams of complexes prepared at different conditions of pH and ionic strength.

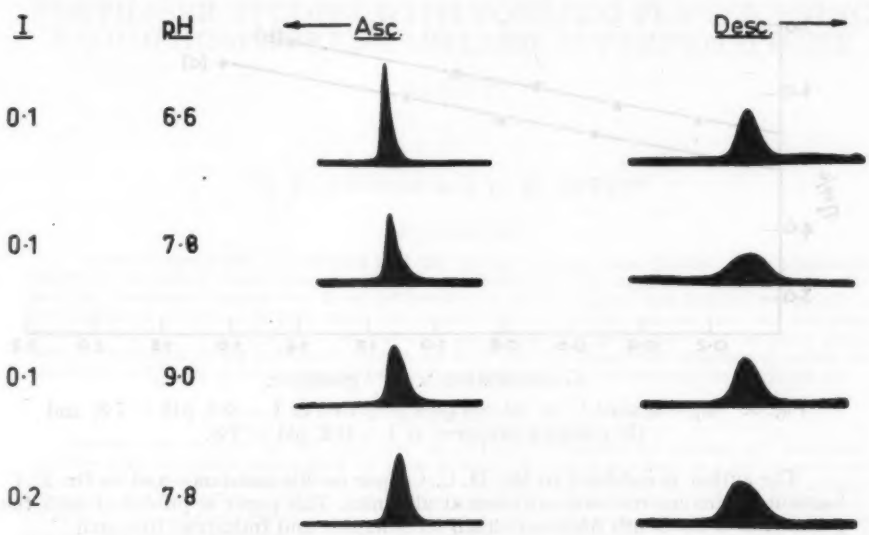

Fig. 3. Electrophoretic diagrams of complexes prepared at different conditions of pH and ionic strength.

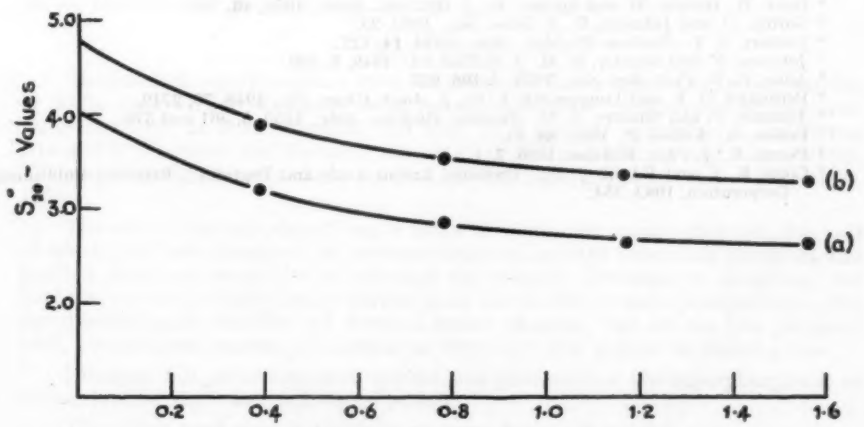

Fig. 4. S°_{20} — values against C for (a) complex prepared at I = 0·1, pH = 7·8 and (b) complex prepared at I = 0·2, pH = 7·8.

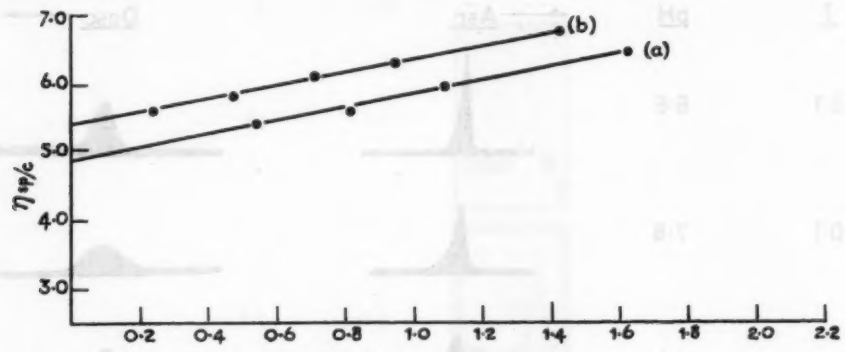

Fig. 5. η_{sp}/c against C for (a) complex prepared at I = 0·1, pH = 7·8, and (b) complex prepared at I = 0·2, pH = 7·8.

The author is indebted to Mr. D. C. Cooper for his assistance and to Dr. P. C. Carman for his interest and criticism at all times. This paper is published with the permission of the South African Council for Scientific and Industrial Research.

National Chemical Research Laboratory,
South African Council for Scientific and Industrial Research,
Pretoria. *Received April* 25, 1955.

REFERENCES

[1] Bull, H. B. and Neurath, H., *J. Biol. Chem.*, 1937, **118**, 163.
[2] Johnson, P. and Joubert, F. J., *J. Polymer Sci.*, 1951, **7**, 605.
[3] Joubert, F. J. and Cooper, D. C., *J. S.A. Chem. Inst.*, 1954, **7**, 99.
[4] Brice, B., Halwer, M. and Speiser, R., *J. Opt. Soc. Amer.*, 1950, **40**, 768.
[5] Goring, D. and Johnson, P., *J. Chem. Soc.*, 1952, 33.
[6] Joubert, F. J., *Biochem. Biophys. Acta.*, 1954, **14**, 127.
[7] Johnson, P. and Shooter, E. M., *J. Colloid Sci.*, 1948, **3**, 539.
[8] Adair, G. S., *Proc. Roy. Soc.*, 1925, **A 108**, 627.
[9] Perlmann, G. E. and Longsworth, L. G., *J. Amer. Chem. Soc.*, 1948, **70**, 2719.
[10] Johnson, P. and Shooter, E. M., *Biochem. Biophys. Acta*, 1950, **5**, 361 and 376.
[11] Polson, A., *Kolloid-Z.*, 1939, **88**, 51.
[12] Perrin, F., *J. Phys. Radium*, 1936, **7**, 1.
[13] Cohn, E. J. and Edsall, J. T., "Proteins, Amino Acids and Peptides", Reinhold Publishing Corporation, 1943, 354.

FERTILISER STUDIES WITH TOBACCO PLANTS USING RADIOPHOSPHORUS-LABELLED SUPERPHOSPHATE

PART V.

by

H. L. PEARSE and L. H. STEIN*

OPSOMMING

Verdere eksperimente in verband met die nuttige opname van fosfaat deur tabakword beskrywe. Gemerkte superfosfaat is op drie versikllende metodes toegedien op grond wat baie arm aan beskikbare fosfaat was. In al die gevalle het die toevoeging van fosfaat 'n toename in fosfaatopname as gevolg gehad, maar die metode van toediening was nie van veel betekenis behalwe in die vroeë groeistadium nie. Bemeste plante het meer grondfosfaat in die latere groeistadium opgeneem as die onbemeste plante. Dit blyk dat vaslegging van toegediende fosfaat nie merkbaar groter was op laat geploegde, as op vroeg geploegde, voorheen onbewerkte grond nie.

SUMMARY

Further experiments on the utilisation of fertiliser phosphate by tobacco are described. Labelled superphosphate was applied by three different placement methods to a soil known to be extremely deficient in available phosphate. In all cases addition of phosphate resulted in increased phosphate uptake but the method of placement was not important except in the early stages of growth. Fertilised plants absorbed more soil phosphate at a late growth stage than did unfertilised plants. Fixation of applied phosphate did not appear to be appreciably greater on late ploughed as compared to early ploughed virgin soil.

INTRODUCTION

An account is given in this paper of further experiments carried out on the utilisation of phosphates by tobacco grown on the phosphate deficient red, sandy clay soil of dolomitic origin, described in a previous publication[1]. The object of these experiments was two-fold, namely (1) to evaluate the importance of microbiological fixation of phosphate in this soil and (2) to determine the effect of fertiliser placement on the utilisation of phosphate by tobacco.

MATERIALS

The labelled superphosphate used was prepared in the usual way in two batches of 20 lb. each at the Research Department of African Explosives and Chemical Industries Ltd., at Modderfontein. The total P_2O_5 content of batches A and B was 20·4 and 20·2 *per cent.* and the water soluble P_2O_5, 19·2 and 18·6 *per cent.*, respectively. The specific activities were of the order of 500 urd/mg. P_2O_5 at the end of November, 1954.

The site of the experiment was a block of virgin red, sandy clay soil, one half of which had been ploughed the previous summer and the other half ploughed and levelled about six weeks before planting the tobacco. Previous to ploughing, the land was carrying a fairly heavy natural grass cover. On the early ploughed land, the incorporated grass stubble had decayed before planting, but on the late ploughed land, considerable amounts of undecayed litter were still present at planting time.

Nitrogen and potassium were applied independently of the superphosphate, as ammonium sulphate and muriate of potash.

The plants used were of the Orinoco type, Yellow Mammoth x Vamorr variety and were approximately ten weeks old at the time of transplanting.

* Present Address: Research Department, African Explosives and Chemical Industries, Limited, P.O. Northrand, Transvaal.

The mechanical composition of the soil used was: clay, 34 *per cent.*, silt, 12 *per cent.* and sand, 54 *per cent.* The pH value (1-1 soil suspension) was 5·9 and the specific conductivity 0·24 $\times$ 10^{-3}ohm^{-1} at 25°C.

The available phosphate, (Morgan) before planting is given in Table I.

TABLE I.

Available Soil Phosphate at Planting.

Depth	Available P_2O_5 p.p.m.	
	Early Ploughed: X	Late Ploughed: Y
1st ft.	9·0	4·0.
2nd ft.	0·0	8·0
3rd ft.	0·0	0·0

EXPERIMENTAL

There were two sites of identical size, one on the early ploughed land (X) and the other on the late ploughed land (Y). On each site there were four plots, each of four treatments, laid out in the randomized block form. There were four control rows, C, which received only potassium and nitrogen equivalent to 800 lb. per morgen of a 4N6K mixture. The other twelve rows were treated with a 4N12P6K mixture at a rate equivalent to 800 lb. per morgen. These twelve consisted of four rows each treated with superphosphate by three different methods of placement, namely (a) mixed with the top two inches of soil in the furrow (P.2), (b) mixed with the top eight inches of soil in the furrow (P.8.), and (c) placed as a band at a depth of six inches to one side of the planting stations (P.6.B). The rows were spaced 5 feet apart and the plants 18 inches apart in the rows.

The fertiliser was applied on the 1st November, 1954, and the tobacco plants were transplanted the following day. Harvesting was carried out by taking four plants from each row 13, 27, 41, 55, 69 and 83 days after planting and these samples are referred to as series 1 to 6. The samples were dried, milled and sub-samples of the milled material taken for analysis.

CHEMICAL AND RADIOMETRIC ANALYSIS

Counting of solutions for radiometric analysis of fertiliser phosphate was carried out in the normal way with an M12 counter (20th Century Electronics). The necessary dilutions were made to avoid coincidence loss and where necessary corrections were applied for density effect, potassium contribution and decay of P^{32}.

Total phosphate in the plant material was determined as described in previous publications[1, 2, 3, 4].

RESULTS

The mean dry weight yield per four plants, at each harvest, together with the results of chemical and radiometric analysis for phosphate in the plant material, are set out in Tables II and III. The percentage of fertiliser phosphate to total phosphate for each treatment at each growth stage is also shown. In the last columns the A value (lb. per morgen available P_2O_5 in the soil), as obtained from the Fried and Dean[5] formula, is given.

TABLE II

Plant Yield and P_2O_5 Concentration: Site X

Series	Days after planting	Treatment	Dry wt. g.	mg. P_2O_5 per g. dry wt.	mg. Fert. P_2O_5 per g. dry wt.	$\frac{\text{Fert.}P_2O_5}{\text{Total}P_2O_5}$ %	"A value" lb. P_2O_5 per morgen
1	13	P.2.	8·9	4·86	1·65	34·9	—
		P.8	7·7	4·55	1·29	26·1	—
		P.6.B	10·1	3·36	0·43	12·8	—
		C.	7·5	4·03	—	—	—
L.S.D. (P = 0·05)			N.S.	N.S.	0·64	12·5	—
2	27	P.2	35·2	6·22	5·25	84·4	18
		P.8	35·6	6·21	4·53	72·6	40
		P.6.B	33·0	5·83	4·99	85·6	16
		C.	12·8	2·44	—	—	—
L.S.D. (P = 0·05)			9·8	0·75	N.S.	N.S.	N.S.
3	41	P.S.	159·1	4·30	3·56	82·8	20
		P.8	161·6	3·44	3·16	91·8	16
		P.6.B	154·3	3·27	2·50	76·4	31
		C.	27·1	2·40	—	—	—
L.S.D. (P = 0·05)			31·9	0·37	0·50	N.S.	N.S.
4	55	P.2	315·3	2·80	2·47	88·2	12
		P.8	355·3	2·74	2·67	97·0	12
		P.6.B	297·3	2·79	1·96	70·2	41
		C.	90·6	2·39	—	—	—
L.S.D. (P = 0·05)			70·2	N.S.	0·37	N.S.	N.S.
5	69	P.2	702·6	1·91	1·52	79·5	25
		P.8	684·6	1·80	1·46	81·1	24
		P.6.B	686·6	2·02	1·62	80·1	24
		C.	162·0	1·90	—	—	—
L.S.D. (P = 0·05)			105·8	N.S.	N.S.	N.S.	N.S.
6	83	P.2	836·6	2·09	1·18	56·4	74
		P.8	998·6	2·24	1·34	59·8	65
		P.6.B	822·6	2·07	1·08	52·1	92
		C	149·3	2·10	—	—	—
L.S.D. (P = 0·05)			195·5	N.S.	N.S.	N.S.	N.S.

TABLE III

Plant Yield and P_2O_5 Concentration: Site Y.

Series	Days after planting	Treatment	Dry wt. g.	mg. P_2O_5 per g. dry wt.	mg. Fert. P_2O_5 per g. dry wt.	Fert.P_2O_5 / TotalP_2O_5 %	"A value" lb. P_2O_5 per morgen
1	13	P.2	7·2	4·12	0·60	14·3	—
		P.8	7·6	4·88	0·81	16·6	—
		P.6.B	6·3	6·04	0·39	6·4	—
		C.	9·7	2·95	—	—	—
L.S.D. (P = 0·05)			N.S.	1·58	N.S.	N.S.	—
2	27	P.2	34·0	6·55	5·20	79·3	24
		P.8	45·8	6·21	4·49	72·3	42
		P.6.B	32·3	5·05	3·76	74·4	34
		C.	17·0	2·35	—	—	—
L.S.D. (P = 0·05)			12·5	0·90	0·74	N.S.	N.S.
3	41	P.2	147·7	4·18	3·42	81·5	21
		P.8	98·4	3·53	2·89	81·8	22
		P.6.B	123·0	3·34	2·50	74·9	34
		C.	30·9	2·14	—	—	—
L.S.D. (P = 0·05)			33·3	0·41	0·51	N.S.	N.S.
4	55	P.2	271·3	3·30	2·57	77·9	28
		P.8	222·0	3·46	2·23	64·4	53
		P.6.B	204·6	2·41	2·05	85·0	20
		C.	63·3	2·29	—	—	—
L.S.D. (P = 0·05)			54·3	N.S.	N.S.	N.S.	N.S.
5	69	P.2	539·3	2·28	1·78	78·0	30
		P.8	486·0	2·07	1·45	70·0	42
		P.6.B	390·0	1·99	1·43	71·8	39
		C.	108·0	2·01	—	—	—
L.S.D. (P = 0·05)			103·4	N.S.	N.S.	N.S.	N.S.
6	83	P.2	776·6	2·07	1·10	52·1	104
		P.8	696·6	2·50	1·16	46·4	112
		P.6.B	760·3	2·06	1·03	50·0	95
		C.	125·0	2·20	—	—	—
L.S.D. (P = 0·05)			166·4	N.S.	N.S.	N.S.	N.S.

The most important findings from Tables II and III are the following:

Growth as measured by dry weight increase, was greatly increased by the application of superphosphate on both the sites.

Up to eight weeks growth on the early ploughed soil, and up to six weeks on the late ploughed soil, mixing of the superphosphate with the top two inches of the soil resulted in a better supply of phosphate to the plants than either the deeper mixing or the band method. The band method of application caused a considerable delay in phosphate absorption on this very phosphate deficient soil. In the later growth stages these differences largely disappeared.

Growth was not so good on the late ploughed soil and all plants on this site exhibited visible symptoms of nitrogen hunger owing to the late incorporation of the grass litter.

On both sites, up to the tenth week of growth (series 5) over 70 *per cent.* of the phosphate intake was derived from the fertiliser phosphate applied. From the tenth to the twelfth week of growth, however, this figure had dropped to about 50 *per cent.* and a very considerable amount of phosphate was at this stage being derived from the soil phosphate reserves.

In Tables IV and V the total phosphate uptake and the fertiliser fraction per four plants at each harvest are shown, together with the difference between these amounts, which gives a figure for soil phosphate absorption for each treatment. In the last columns the percentage recovery of the applied fertiliser phosphate is given for the sixth sampling.

TABLE IV

Total fertilizer and soil phosphate uptake: Site X.

Series	Days after planting	Treatment	Total P_2O_5 uptake g.	Fert. P_2O_5 g.	Soil P_2O_5 g.	Recovery of P_2O_5 %
1	13	P.2	0·043	0·014	0·029	—
		P.8	0·035	0·010	0·025	—
		P.6.B	0·033	0·004	0·029	—
		C	0·029	—	0·029	—
L.S.D. (P = 0·05)			N.S.	0·005	N.S.	—
2	27	P.2	0·217	0·183	0·034	—
		P.8	0·218	0·163	0·055	—
		P.6.B	0·188	0·163	0·025	—
		C	0·031	—	0·031	—
L.S.D. (P = 0·05)			0·054	N.S.	N.S.	—
3	41	P.2	0·688	0·569	0·119	—
		P.8	0·554	0·508	0·046	—
		P.6.B	0·511	0·395	0·116	—
		C	0·065	—	0·065	—
L.S.D. (P = 0·05)			0·151	N.S.	N.S.	—
4	55	P.2	0·868	0·780	0·088	—
		P.8	0·919	0·811	0·108	—
		P.6.B	0·837	0·587	0·250	—
		C	0·218	—	0·218	—
L.S.D. (P = 0·05)			0·207	N.S.	N.S.	—
5	69	P.2	1·338	1·075	0·263	—
		P.8	1·232	0·994	0·238	—
		P.6.B	1·384	1·105	0·279	—
		C	0·257	—	0·257	—
L.S.D. (P = 0·05)			0·249	N.S.	N.S.	—
6	83	P.2	1·761	1·000	0·761	12·1
		P.8	2·224	1·354	0·870	16·4
		P.6.B	1·708	0·877	0·831	10·6
		C	0·314	—	0·314	—
L.S.D. (P = 0·05)			0·555	N.S.	0·336	N.S.

TABLE V

Total fertilizer and soil phosphate uptake: Site Y.

Series	Days after planting	Treatment	Total P_2O_5 uptake g.	Fert. P_2O_5 g.	Soil P_2O_5 g.	Recovery of P_2O_5 %
1	13	P.2	0·030	0·004	0·026	—
		P.8	0·035	0·005	0·030	—
		P.6.B	0·037	0·002	0·035	—
		C	0·029	—	0·029	—
L.S.D. (P = 0·05)			N.S.	N.S.	N.S.	—
2	27	P.2	0·220	0·176	0·044	—
		P.8	0·287	0·200	0·087	—
		P.6.B	0·159	0·124	0·035	—
		C	0·040	—	0·040	—
L.S.D. (P = 0·05)			0·070	N.S.	N.S.	—
3	41	P.2	0·619	0·505	0·114	—
		P.8	0·339	0·280	0·059	—
		P.6.B	0·408	0·307	0·101	—
		C	0·066	—	0·066	—
L.S.D. (P = 0·05)			0·118	0·119	N.S.	—
4	55	P.2	0·874	0·687	0·187	—
		P.8	0·772	0·490	0·282	—
		P.6.B	0·486	0·416	0·070	—
		C	0·158	—	0·158	—
L.S.D. (P = 0·05)			0·230	0·148	N.S.	—
5	69	P.2	1·219	0·948	0·261	—
		P.8	0·985	0·688	0·297	—
		P.6.B	0·762	0·544	0·218	—
		C	0·216	—	0·216	—
L.S.D. (P = 0·05)			0·148	0·190	N.S.	—
6	83	P.2	1·642	0·864	0·778	10·5
		P.8	1·760	0·820	0·940	10·0
		P.6.B	1·582	0·791	0·791	9·6
		C	0·274	—	0·274	—
L.S.D. (P = 0·05)			0·552	N.S.	0·278	N.S.

It is clear that up to the fifth series, ten weeks after planting, the applications of superphosphate have not significantly increased the amount of soil phosphate taken up by the tobacco. Thus, on both sites, the control plants, which did not receive fertiliser phosphate have taken up as much soil phosphate as the fertilised plants. From the tenth to the twelfth week, however, this position shows a sharp change and the fertilised plants have absorbed considerably more soil phosphate than the unfertilised plants.

The percentage recovery of applied phosphate was about ten *per cent.*, with a tendency for recovery to be slightly higher on the early ploughed soil.

The total nitrogen content of the tobacco plants at the sixth sampling was determined and is shown in Table VI.

TABLE VI

Total Nitrogen Content of Tobacco Plants: Series 6.

Treatment	Dry Weight g.		$\frac{\text{Total N}}{\text{Dry Weight}}$ %	
	X	Y	X	Y
P. 2	836·6	776·6	1·92	1·64
P. 8	998·6	696·6	1·99	1·71
P. 6.B	822·6	760·3	2·01	1·72
C	149·3	125·0	2·42	2·38
L.S.D. (0·05)	195·5	166·4	0·28	0·37

The higher nitrogen content and better growth of the plants from the X group is evident and also the effect of phosphate deficiency in causing nitrogen accumulation in the plants, from both sites.

A very curious feature which has now been observed to occur for two seasons on this soil, is the fact that from the tenth week onward after planting out, the control plants which up to that time had made very little growth and showed acute symptoms of phosphate deficiency, began to make considerable growth. This occurs at the time when the plants receiving phosphate also begin to absorb considerably greater quantities of phosphate from the soil reserves. In order to obtain more information on this point a further sampling was made at the 14th week of growth (series 7) and analysed for total phosphate content. The results are shown in Table VII.

TABLE VII

Phosphate Uptake and Increase in Dry Weight: 12th to 14th Week.

SITE X. PLOUGHED EARLY

Treatment	Dry Weight g.			Total P_2O_5 mg.		
	12th Week	*14th Week*	*Increase*	*12th Week*	*14th Week*	*Increase*
P. 2	837	1382	545	1761	3593	1832
P. 8	999	1188	189	2224	2877	653
P. 6.B	823	1143	320	1708	2625	917
C	149	533	384	314	1295	981
L.S.D.(0·05)	196	309	—	555	777	—

SITE Y. PLOUGHED LATE

Treatment	Dry Weight g.			Total P_2O_5 mg.		
	12th Week	*14th Week*	*Increase*	*12th Week*	*14th Week*	*Increase*
P. 2	777	1001	224	1642	2288	646
P. 8	697	879	182	1760	2166	406
P. 6.B	760	812	52	1582	1844	262
C	125	389	264	274	854	580
L.S.D.(0·05)	166	265	—	552	683	—

It is evident from Table VII that even the control plants which received no phosphate fertiliser, have absorbed very considerable amounts of phosphate from the soil at this late growth stage and have in fact made reasonable growth and reached the flowering stage.

DISCUSSION OF RESULTS

On this phosphate deficient soil it is clear that growth of tobacco has been very much improved by the application of superphosphate. Except in the early growth stages, where the band method of application resulted in poorer growth and phosphate uptake than did incorporation with the topsoil, the method of application has not markedly affected either growth or phosphate absorption. Within the scope of this experiment therefore, incorporation of the superphosphate with the topsoil in the furrow shortly before planting has given as good a result as any other method.

Growth was poorer on the late ploughed soil than on the early ploughed, undoubtedly owing largely to nitrogen deficiency caused by the incorporation of considerable amounts of undecayed grass stubble before planting, in the former. There is little evidence for any very appreciable difference in microbiological fixation of phosphate on the two sites, although this effect if it occurred was certainly overshadowed by the difference in nitrogen availability. It is possible that a clearer decision on this point could be obtained by providing a higher level of applied nitrogen.

The fact that a peak absorption of phosphate by tobacco occurs at the late flowering stage is well known, but the source of phosphate for the control plants on this very deficient soil at this stage remains obscure. These plants had made very little growth at all up to ten weeks from planting out and exhibited visible symptoms of extreme phosphate deficiency and only after this stage did they begin to make appreciable growth. Soil samples were taken for analysis from the control plots at the thirteenth week and these showed that the available phosphate status had not appreciably changed from the beginning of the experiments, as assessed by this method. The results were as follows:— X. 1st foot, 12·5 p.p.m., 2nd foot, 0·0 p.p.m.: Y. 1st foot, 0·0 p.p.m., 2nd foot, 0·0 p.p.m. The only possible explanation therefore appears to be that at a certain stage of development the tobacco plant can absorb considerable amounts of phosphate, even from a soil very deficient in phosphate, owing either to the development of a very extensive root system, or to some change in the absorbing capacity of the roots. In any case this point requires further investigation.

CONCLUSIONS

The plants receiving fertiliser phosphate, irrespective of the method of placement, absorbed more phosphate from the soil than those receiving no added phosphate; this difference became apparent from the tenth week after planting out. This result, coupled with the fact that the greatest uptake of fertiliser phosphate has again been shown to occur the first few weeks after planting out, supports the view that the most efficient phosphate fertilisation of tobacco is achieved by supplying a readily available source of phosphate in the furrow just before planting, combined with holding the soil phosphate level reasonably high. In practice, this could probably be achieved by broadcasting and ploughing in 1 to 2 tons per morgen of rock phosphate in the winter, followed by an application of from 600 to 800 lb. of superphosphate per morgen in the furrow shortly before planting out.

The authors are indebted to Messrs. D. P. Botha, L. Kriek and I. J. Roth for their valuable assistance.

This paper is published by permission of the Director of the Central Tobacco Research Station and of the South African Council for Scientific and Industrial Research.

Central Tobacco Research Station, Rustenburg.
National Chemical Research Laboratory,
S.A. Council for Scientific and Industrial Research, Pretoria.

Received, May 25, 1955.

REFERENCES

[1] Stein, L. H. and Pearse, H. L., *This Journal*, 1954, **7**, 125.
[2] Marais, J. S. C. and Stein, L. H., *Agric. Ed. and Res. Science Series*, No. 9, Bulletin No. 213, 1952.
[3] Stein, L. H. and Marais, J. S. C., *S.A. Ind. Chemist*, 1952, **6**, 147.
[4] Pearse, H. L. and Stein, L. H., *This Journal*, 1953, **6**, 25.
[5] Fried, M. and Dean, L. A., *Soil Science*, 1952, **73**, 263.

ULTRACENTRIFUGE STUDIES ON SEED PROTEINS OF THE FAMILY LEGUMINOSAE

PART I—YELLOW LUPIN SEED (*LUPINUS LUTEUS*) PROTEINS

by

F. J. JOUBERT

OPSOMMING

Die globuliene van geel lupiensaad is in die ultrasentrifuge ondersoek. Die drie verskillende globuliene bevat in gesuiwerde lupiensaad is deur ammoniumsulfaatfraksionasie geskei. Die hoëmolekulêrgewig-globulien kan omkeerbaar dissosieer word. 'n Geringe assosiasie is vir die tweede globulin van lupiensaad in sekere buffers waargeneem.

SUMMARY

The globulins of yellow lupin seed were examined in the ultracentrifuge. Purified lupin seed contains three different globulins which have been separated by ammonium sulphate fractionation. The high molecular weight globulin can be reversibly dissociated. A slight association was found in certain buffers for the second globulin of yellow lupin seed.

Published work on the proteins of yellow lupin seed includes an early paper by Osborne and Campbell[1]. More recently Danielsson[2] has reported ultracentrifugal sedimentation constants for two globulins of yellow lupin seed and Petri and Stavermann[3] described the preparation and chemical modification of membranes from the globulins. A physico-chemical study on the proteins of the presumably closely similar blue lupin (*Lupinus angustifolius*) was carried out by Joubert[4].

The present investigation is mainly concerned with the fractionation of the globulins in yellow lupin seed meal, and the ultracentrifugal examination of these components under different conditions of pH and ionic strength. Preliminary results on yellow lupin seed proteins have already been published[5].

METHODS

Sedimentation studies were carried out at a protein concentration of *ca.* 1 *per cent.* in a Spinco electrically driven ultracentrifuge manufactured by Messrs. Specialised Instrument Corporation, Belmont, California. All the runs were performed at *ca.* 60,000 r.p.m., equivalent to a centrifugal force of *ca.* 250,000 g. Dialysis of protein solutions was routinely performed in a slowly rotating cellophane bag against a large volume of the required buffer solution. Dialysis was carried out for 24 hours with 2 or 3 changes of buffer.

Electrophoresis was carried out in a Tiselius electrophoretic apparatus manufactured by Messrs. Hilger Watts Ltd., using a medium U-tube equipped with a long centre section. Because of low protein solubility at 0—4°C, electrophoresis was carried out at 20°C, field strengths employed being limited accordingly[6].

PREPARATION OF PROTEINS

It has previously been observed[4] that the coloured constituents occurring in lupin seed interact with the proteins to form new electrophoretic components. It was therefore considered necessary to attempt to remove the colouring matter from the meal before the proteins were extracted. Complete removal of these impurities was effected by repeated extraction of the decorticated and defatted meal with 50 — 50 ethanol-water mixture and cold water using a Waring Blendor as described[4]. The purified meal contains only the globulin components as the albumin portion is removed in the water wash[5].

The proteins of the purified meal were completely extracted with three separate volumes of 10 *per cent.* sodium chloride over a period of 24 hours at 4°C. The final

protein extract was centrifuged clear at 2,500 r.p.m. The extracted proteins were precipitated by adding ammonium sulphate to 85 *per cent.* saturation. Fig. 1 (a) gives sedimentation diagrams of this preparation in phosphate buffer of ionic strength (I) = 0·31, pH = 7·0. Three major components of sedimentation constants 11·6, 7·4 and 2·0 Svedberg Units (S.U.) (designated as the $S_{11\cdot6}$, $S_{7\cdot4}$ and $S_{2\cdot0}$ components were observed.

In an attempt to fractionate the three globulins of yellow lupin seed, successive amounts of saturated ammonium sulphate were added to a 10 *per cent.* sodium chloride purified lupin seed extract. The fractions obtained at 40 ,50, 60 and 85 *per cent.* saturation with ammonium sulphate were examined in the ultracentrifuge in buffer I = 0·31, pH = 7·0. Whereas the 40 and 50 *per cent.* fractions (Fig. 1 (b) and 1 (c)) contained a major $S_{11\cdot6}$ component and minor concentrations of the $S_{7\cdot4}$ component, the 60 *per cent.* fraction (Fig. 1 (d)) contained a major $S_{7\cdot4}$ component and small concentrations of the $S_{11\cdot6}$ and $S_{2\cdot0}$ components. Similarly the 85 *per cent.* fraction (Fig. I (e)) contained a major $S_{2\cdot0}$ component and a minor concentration of the $S_{7\cdot4}$ component. Since different components were found at different degrees of saturation with ammonium sulphate, it would appear that this method can be used for the fractionation of the three globulins.

As a result of the experience gained by the above mentioned experiments, the proteins present in yellow lupin seed meal were fractionated as outlined in Fig. 2. When the 10 *per cent.* sodium chlordie protein extract was 47 *per cent.* saturated with ammonium sulphate, about 35 *per cent.* of the proteins were precipitated (Fraction A). On the addition of ammonium sulphate to 64 *per cent.* saturation a further 25 *per cent.* of the proteins were precipitated (Fraction B) and at 85 *per cent.* saturation the residual proteins (Fraction C). In a further purification Fraction A was reprecipitated at 45 *per cent.* saturation and Fraction B in the range 47 — 62 *per cent.* saturation with ammonium sulphate.

Fig. 3 gives sedimentation diagrams in buffer I = 0·31, pH = 7·0 and Fig. 4 electrophoretic diagrams in buffer I = 0·1, pH = 8·8 of the fractions outlined in Fig. 2. For Fractions A,

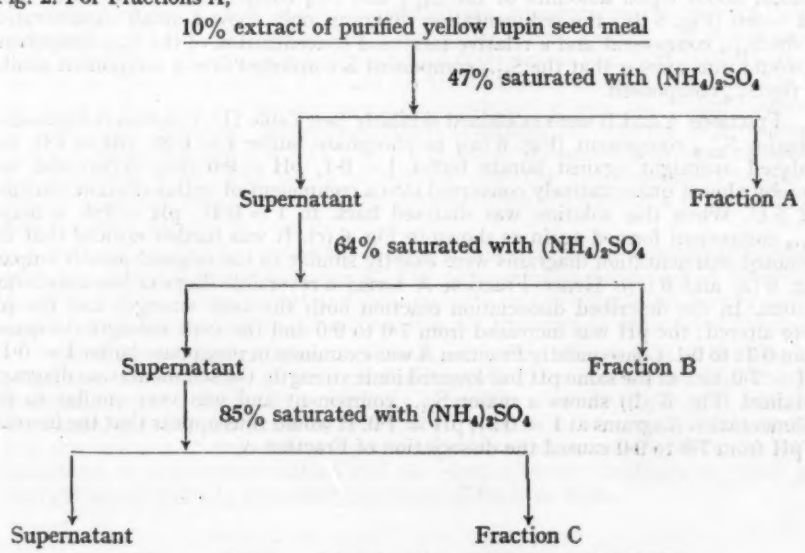

Fig. 2. Scheme of fractionation of lupin seed globulins.

B and C major $S_{11\cdot6}$, $S_{7\cdot4}$ and $S_{2\cdot0}$ components were respectively found in the ultracentrifuge, and, as shown in Fig. 3, these fractions were reasonably pure. Similar indications were found for Fractions A and B from the electrophoretic diagrams (Fig. 4), but the electrophoretic diagram of Fraction C showed the presence of two components. Electrophoretic mobilities of the different fractions are given in Table I.

TABLE I

Electrophoretic Mobilities of Yellow Lupin Seed fractions at 20°C, in buffer I = 0·1, pH = 8·8

Fraction	Mobility × 10^{-4} cm.^{2} sec.$^{-1}$ volt^{-1}	
	Descending	Ascending
Fraction A ($S_{11\cdot6}$)	1·14	1·25
Fraction B ($S_{7\cdot4}$)	0·76	0·86
Fraction C ($S_{2\cdot0}$)	1·39*	1·57*

* Major component.

DISSOCIATION

When the globulins of purified lupin seed meal were examined in different buffers, the relative proportion of the $S_{11\cdot6}$ and $S_{7\cdot4}$ components were significantly changed. Thus at I = 0·31, pH = 7·0 the sedimentation diagrams (Fig. 5 (a)) contain about equal amounts of the $S_{11\cdot6}$ and $S_{7\cdot4}$ components, while at I = 0·1, pH = 9·0 (Fig. 5 (b)) the sedimentation diagrams only show a small concentration of the $S_{11\cdot6}$ component and a relative increased concentration of the $S_{7\cdot4}$ component. It would thus appear that the $S_{11\cdot6}$ component is converted into a component similar to the $S_{7\cdot4}$ component.

Fractions A and B were examined similarly (see Table II). Fraction A containing a major $S_{11\cdot6}$ component (Fig. 6 (a)) in phosphate buffer I = 0·31, pH = 7·0, was dialysed overnight against borate buffer I = 0·1, pH = 9·0 (Fig. 6 (b)) and was thereby almost quantitatively converted into a component of sedimentation constant 7·2 S.U. When this solution was dialysed back to I = 0·31, pH = 7·0, a major $S_{11\cdot6}$ component formed again as shown in Fig. 6 (c). It was further noticed that the obtained sedimentation diagrams were exactly similar to the original ones (Compare Fig. 6 (a) and 6 (c)). Hence Fraction A forms a reversible dissociation-association system. In the described dissociation reaction both the ionic strength and the pH were altered; the pH was increased from 7·0 to 9·0 and the ionic strength decreased from 0·31 to 0·1. Consequently Fraction A was examined in phosphate buffer I = 0·11, pH = 7·0, i.e., at the same pH but lowered ionic strength, the sedimentation diagrams obtained (Fig. 6 (d)) shows a major $S_{11\cdot6}$ component and was very similar to the sedimentation diagrams at I = 0·31, pH = 7·0. It would thus appear that the increase in pH from 7·0 to 9·0 caused the dissociation of Fraction A.

TABLE II

Sedimentation constants of major components of Fractions A and B in different buffers.

Fraction	I	pH	Sedimentation constants (S_{20}—values)	
Fraction A	0·31	7·0	11·6	
	0·1	9·0		7·2
Dialysed back to:	0·31	7·0	11·8	
	0·1	3·6		6·8
Dialysed back to:	0·31	7·0	12·0	
	0·11	7·0	11·8	
Fraction B	0·31	7·0		7·3
	0·1	3·6		6·8
	0·1	9·0		7·9
	0·11	7·0		8·1

The dissociation of Fraction A was also examined at a pH below the iso-electric point of the globulin. Fig. 6 (e) containing a major $S_{11\cdot6}$ component gives the original sedimentation diagram of Fraction A in buffer of I = 0·31, pH = 7·0. This solution was dialysed overnight against acetate buffer I = 0·1, pH = 3·6 (Fig. 6 (f)). The $S_{11\cdot6}$ component is hereby quantitatively converted into a component of sedimentation constant 6·8 S.U. When this solution was dialysed back to I = 0·31, pH = 7·0, the $S_{11\cdot6}$ component formed again and as shown in Fig. 6 (g) the sedimentation diagrams were very similar to the original ones.

Fig. 7 (a), (b), (c) and (d) contain respectively sedimentation diagrams of Fraction B in buffers of I = 0·31, pH = 7·0; I = 0·1, pH = 3·6; I = 0·1, pH = 9·0 and I = 0·11, pH = 7·0. Whereas the sedimentation diagrams of Fig. 7 (a) and (b) are very similar the, diagrams of Fig. 7 (c) and (d) are somewhat different. The peaks in both cases are rather asymmetric and show a faster advancing edge, particularly noticeable in Fig. 7 (d). Similarly the sedimentation constants of Fraction B in buffers of I = 0·1, pH = 9·0 and I = 0·11, pH = 7·0 (Table II) were higher than in buffer of I = 0·31, pH = 7·0. This seems to indicate that the $S_{7\cdot4}$ component is partially associated into a component of higher sedimentation constant at I = 0·1, pH = 9·0 and I = 0·11, pH = 7·0.

It is noticed (Table II) that the sedimentation constant of dissociated Fraction A is very similar to that of Fraction B. The sedimentation behaviour of Fractions A and B in buffers of varying pH and ionic strength on the other hand, is very different and it would thus appear that Fraction B is not the same as dissociated Fraction A.

When the proteins of yellow lupin seed are compared with that of the blue lupin previously reported on [4], it is found that in both cases the high molecular weight globulin (Fraction A) could be similarly reversibly dissociated. For the blue lupin the second globulin (Fraction B) was stable to variation of pH and ionic strength. For this fraction of the yellow lupin a slight association was found under certain conditions. It was further noticed that the electrophoretic mobilities of yellow lupin seed globulins (Table I) were similar to those of the blue lupin.

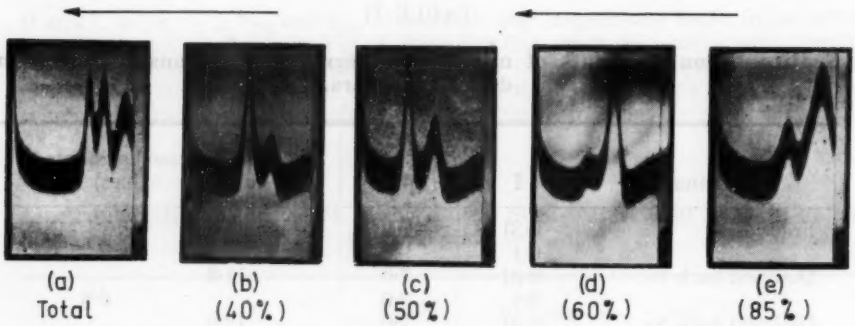

Fig. 1. Sedimentation diagrams of yellow lupin seed globulins in buffer I = 0·31, pH = 7·0.

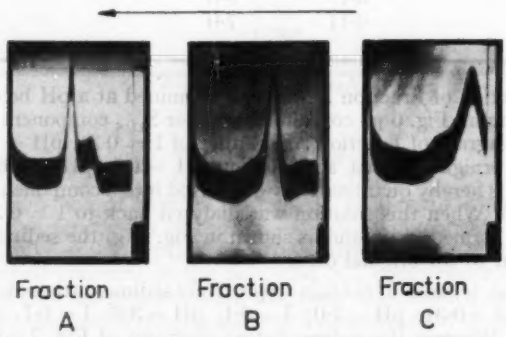

Fig. 3. Sedimentation diagrams of yellow lupin seed protein fractions in buffer I = 0·31, pH = 7·0.

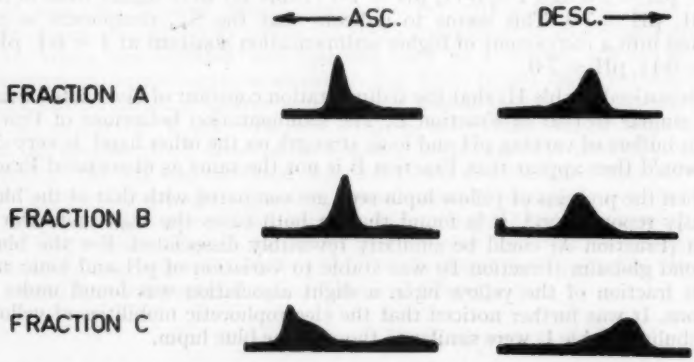

Fig. 4. Electrophoretic diagrams of yellow lupin seed protein fractions in buffer I = 0·1, pH = 8·8.

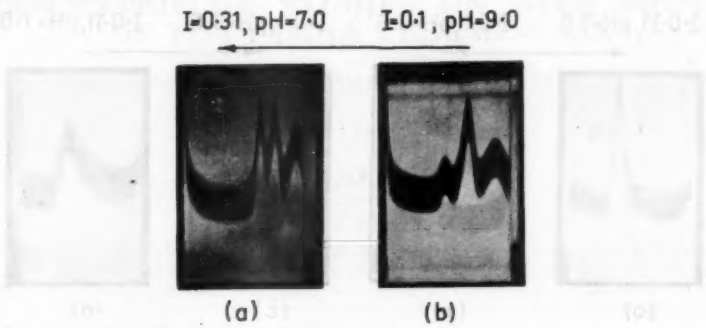

Fig. 5. Sedimentation diagrams of yellow lupin seed globulins in different buffers.

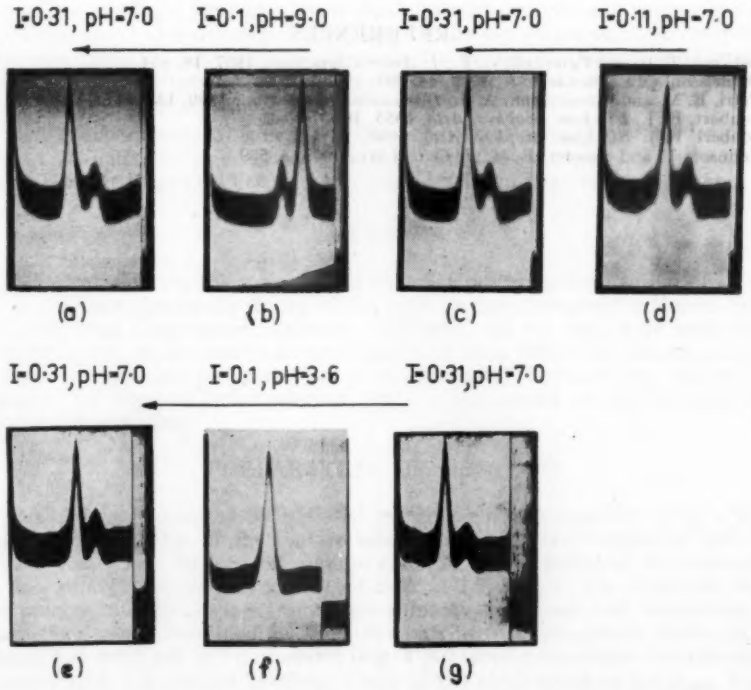

Fig. 6. Sedimentation diagrams of Fraction A in different buffers.

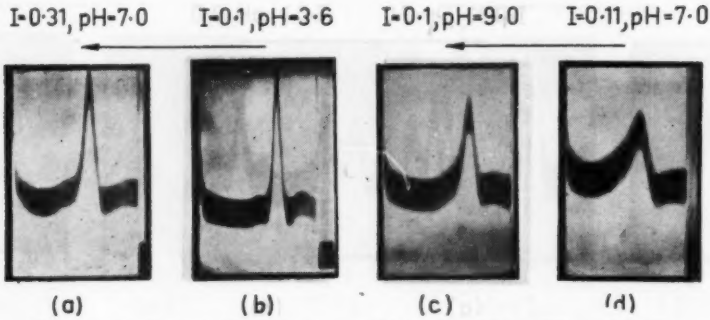

Fig. 7. Sedimentation diagrams of Fraction B in different buffers.

This paper is published with the permission of the South African Council for Scientific and Industrial Research.

National Chemical Research Laboratory,
Council for Scientific and Industrial Research,
Pretoria.

Received, July 4, 1955.

REFERENCES

[1] Osborne, T. B. and Campbell, G. F., *J. Amer. Chem. Soc.*, 1897, **19**, 454.
[2] Danielsson, C. E., *Biochem. J.*, 1949, **44**, 387.
[3] Petri, E. M. and Stavermann, A. J., *Discussions Farad. Soc.*, 1953, **13**, 151.
[4] Joubert, F. J., *Biochem. Biophys. Acta*, 1955, **16**, 370.
[5] Joubert, F. J. *Biochem. Biophys. Acta*, 1955, **17** 444.
[6] Johnson, P. and Shooter, E. M., *J. Colloid Sci.*, 1948, **3**, 539.

ULTRACENTRIFUGE STUDIES ON SEED PROTEINS OF THE FAMILY LEGUMINOSAE

PART II—PEA PROTEINS (*PISUM SATIVUM*)

by

F. J. JOUBERT

OPSOMMING

Die globuliene van ertjies is fraksioneer deur gebruik te maak van die metode beskryf deur Danielsson[2]. Die verskillende globuliene is in die ultrasentrifuge in verskeie buffers ondersoek. Die hoëmolekulêrgewig-globulien toon geen verandering in buffers van verskillende pH en ioniese sterkte nie Die tweede globulin kan egter omkeerbaar assosieer word. Hierdie assosiasiereaksie word deur 'n lae ioniese sterkte en lae pH begunstig.

SUMMARY

Pea globulins were separated according to the method described by Danielsson[2]. The different globulins were examined in the ultracentrifuge in various buffers. The high molecular weight globulin is stable to changes of pH and ionic strength. The second globulin on the other hand can be reversibly associated. Association is favoured by low ionic strength and low pH.

Osborne and Campbell[1] found that the globulin portion of pea protein could be separated into three fractions of different solubility and coagulation properties. Using ultracentrifugal methods, Danielsson[2] isolated two globulin components from peas. Danielsson[2] also developed a method for the separation of these components, which were indentical with vicilin and legumin first studied by Osborne and Campbell[1]. All Danielsson's[2] ultracentrifugal measurements were carried out only in phosphate buffer of ionic strength 0·31, pH = 7·0.

In the experiments which will be described, Danielsson's[2] method for the preparation of vicilin and legumin has been used, and these components were examined in the ultracentrifuge at different conditions of pH and ionic strength.

METHODS

Sedimentation studies were carried out at a protein concentration of *ca.* 1 *per cent.* in a Spinco electrically driven ultracentrifuge manufactured by Messrs. Specialised Instrument Corporation, Belmont, California. All the runs were performed at *ca.* 60,000 r.p.m., equivalent to a centrifugal force of *ca.* 250,000 g. Dialysis of protein solutions was routinely performed in a slowly rotating cellophane bag against a large volume of the required buffer solution. Dialysis was carried out for 24 hours with 2 or 3 changes of buffer.

PREPARATION OF PROTEINS

Pea meal was defatted by repeated extraction with hexane by using a Waring Blendor. The proteins of the oil-free meal were completely extracted with three separate volumes of 10 *per cent.* sodium chloride over a period of 24 hours at 4°C. The final protein extract was centrfuged clear at 2,500 r.p.m. The extracted proteins were precipitated by adding ammonium sulphate to 85 *per cent.* saturation. This preparation, when examined in the ultracentrifuge in phosphate buffer of ionic strength I = 0·31, pH = 7·0, revealed (Fig. 1 (a)) three components of sedimentation constants 12·3, 7·2 and 2·0 Svedberg Units (S.U.) (designated as the $S_{12\cdot3}$, $S_{7\cdot2}$ and $S_{2\cdot0}$ components).

Fractionation of the protein components was carried out according to a slightly modified form of the procedure described by Danielsson[2]. The scheme of fractionation is outlined in Fig. 2.

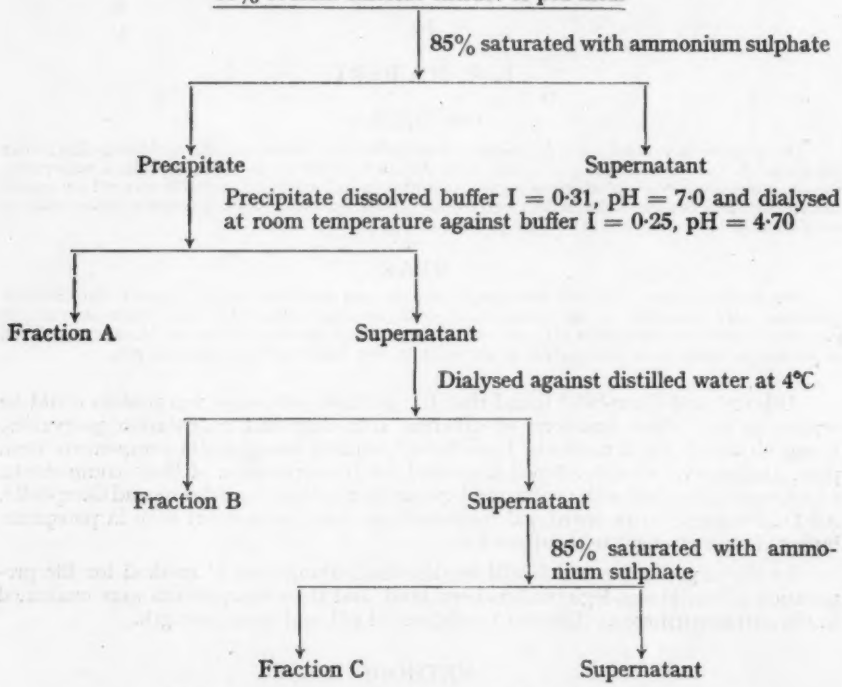

Fig. 2. Scheme of fractionation of pea proteins.

The proteins extracted from pea meal were precipitated by adding ammonium sulphate to 85 *per cent.* saturation. The resulting precipitate was dissolved and dialysed against phosphate buffer I = 0·31, pH = 7·0, centrifuged clear and then dialysed for *ca.* 24 hours at room temperature against an acetate buffer of I = 0·25, pH = 4·70. The precipitate which formed during this dialysis was centrifuged off (Fraction A) and the supernatant was dialysed against distilled water at 4°C and another precipitate (Fraction B) formed. When the supernatant of Fraction B was saturated to 85 *per cent.* with ammonium sulphate, Fraction C was precipitated.

Fig. 1 (b), (c) and (d) give sedimentation diagrams in buffer of I = 0·31, pH = 7·0 of the fractions outlined in Fig. 2. For Fractions A and B major $S_{12\cdot3}$ and $S_{7\cdot2}$ components corresponding to Danielsson's[2] legumin and vicilin, respectively, were found and as shown these components were reasonably pure. Fraction C on the other hand contained major $S_{7\cdot2}$, $S_{4\cdot0}$ and $S_{1\cdot6}$ components.

Examination of Fractions A and B in different buffers.

It was observed that when pea proteins were examined in different buffers, some variation in the relative proportion of the $S_{12\cdot3}$ and $S_{7\cdot2}$ components occurred.

Thus at I = 0·31, pH = 7·0, the sedimentation diagrams (Fig. 3 (a)) contain a larger proportion of the $S_{7\cdot2}$ component, while at I = 0·1, pH = 9·0 (Fig. 3 (b)) the sedimentation diagrams contain about equal amounts of both the $S_{12\cdot3}$ and $S_{7\cdot2}$ components.

Similarly Fractions A and B were examined in different buffers (see Table I).

TABLE I

Sedimentation constants of major components of Fractions A and B in different buffers.

Fraction	I	pH	Sedimentation constants (S°_{20}—values)	
Fraction A	0·51	7·0	11·3	
	0·31	7·0	12·2	
	0·11	7·0	13·1	
	0·1	9·0	12·3	
Fraction B	0·31	7·0		7·1
	0·1	9·0	10·7	7·3
Dialysed back to:	0·31	7·0		7·2
	0·3	9·0		7·0
	0·31	7·0		7·1
	0·11	7·0	10·9	7·3
Dialysed back to:	0·31	7·0		7·2
	0·51	7·0		6·8

Fig. 4 (a), (b), (c) and (d) contain respectively sedimentation diagrams of Fraction A in buffers of I = 0·51, pH = 7·0; I = 0·31, pH = 7·0; I = 0·11, pH = 7·0 and I = 0·1, pH = 9·0. Whereas no significant change was observed in the sedimentation diagrams, a slight variation was found in the sedimentation constants (Table I). Thus at the same pH (7·0) and different ionic strengths the sedimentation constants increase with decreasing salt concentrations.

Fig. 5 (a) showing a major $S_{7\cdot2}$ component gives the sedimentation diagram of Fraction B in phosphate buffer I = 0·31, pH = 7·0. When this solution was dialysed overnight against borate buffer I = 0·1, pH = 9·0, the $S_{7\cdot2}$ component is partially converted into a component of 10·7 S.U. (Fig. 5 (b)). Next this solution was dialysed back to I = 0·31, pH = 7·0 and, as shown in Fig. 5 (c), the $S_{7\cdot2}$ component was formed again and the obtained sedimentation diagrams were exactly similar to the original ones (compare Fig. 5 (a) and (c)). Hence Fraction B forms a reversible association-dissociation system. To cause the association of Fraction B both the salt concentration and pH were varied; the pH was increased from 7·0 to 9·0 and the ionic strength lowered from 0·31 to 0·1. Consequently Fraction B was examined in borate buffer I = 0·3, pH = 9·0, the sedimentation diagrams (Fig. 5 (d)) show a major $S_{7\cdot2}$ component and were very similar to the sedimentation diagram at I = 0·31, pH = 7·0. Thus it would appear that in the described experiment, the decrease in ionic strength from 0·31 to 0·1 caused the association of Fraction B.

This association reaction was also examined at pH = 7·0 and low ionic strength. When a solution of Fraction B in buffer of I = 0·31, pH = 7·0 (Fig. 5 (a)) was dialysed overnight against phosphate buffer I = 0·11, pH = 7·0, the sedimentation diagrams of Fig. 5 (e) were obtained. As shown the $S_{7\cdot2}$ component is hereby partially converted into a component of 10·9 S.U. This solution was dialysed back to I = 0·31, pH = 7·0, the $S_{7\cdot2}$ formed again (Fig. 5 (f)) and the sedimentation diagrams obtained were very

similar to the original ones. When the sedimentation diagrams of Fig. 5 (b) and (e) are compared, it is found that a relative larger proportion of the $S_{10\cdot9}$ component was formed at I = 0·11, pH = 7·0 than at I = 0·1, pH = 9·0. It would thus appear that the association of Fraction B is favoured not only by a low salt concentration but also to some extent by a low pH. As shown in Fig. 5 (g) no change in the sedimentation diagrams of Fraction B was observed in buffer of I = 0·51, pH = 7·0.

The sedimentation constant of associated Fraction B is somewhat lower than that of Fraction A (Table I). It was also noticed that the sedimentation behaviour of Fractions A and B in various buffers is very different. It would thus appear that associated Fraction B is not the same as Fraction A.

It has been observed that the high molecular weight globulin (Fraction A) of yellow lupin seed could be reversibly dissociated (Part I). Under similar conditions the high molecular weight globulin of peas did not show such a dissociation. The second globulin of yellow lupin seed (Fraction B) showed signs of an association reaction in certain buffers. This association was very much more prominent for the second globulin of peas. Both lupin seed and peas belong to the family Leguminosae, and it was noticed that the sedimentation constants of the individual components of both are of the same order. The described study in which the components were examined at different pHs and ionic strengths, indicated the difference between components of similar sedimentation constants of yellow lupin seed and peas.

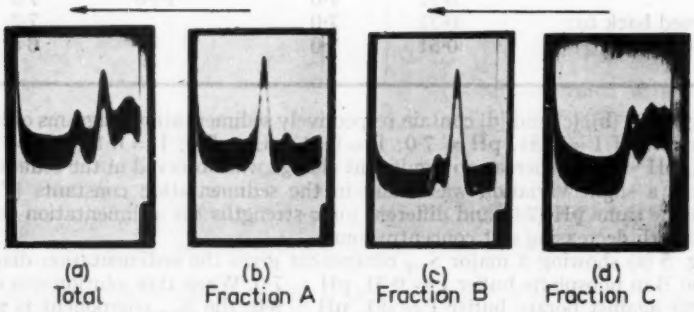

Fig. 1. Sedimentation diagrams of pea proteins in buffer I = 0·31, pH = 7·0.

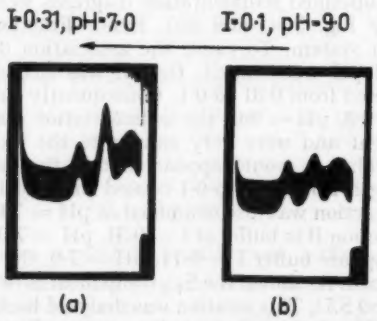

Fig. 3. Sedimentation diagrams of pea proteins in different buffers.

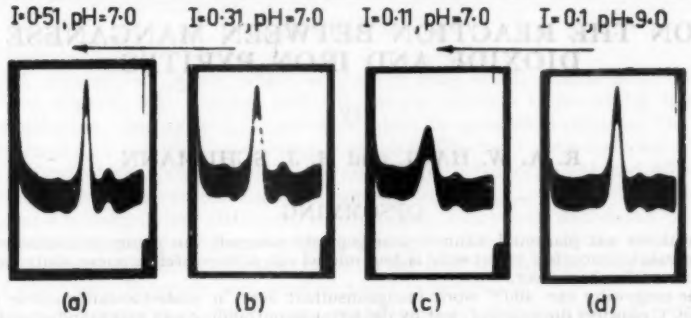

Fig. 4. Sedimentation diagrams of fraction A in different buffers.

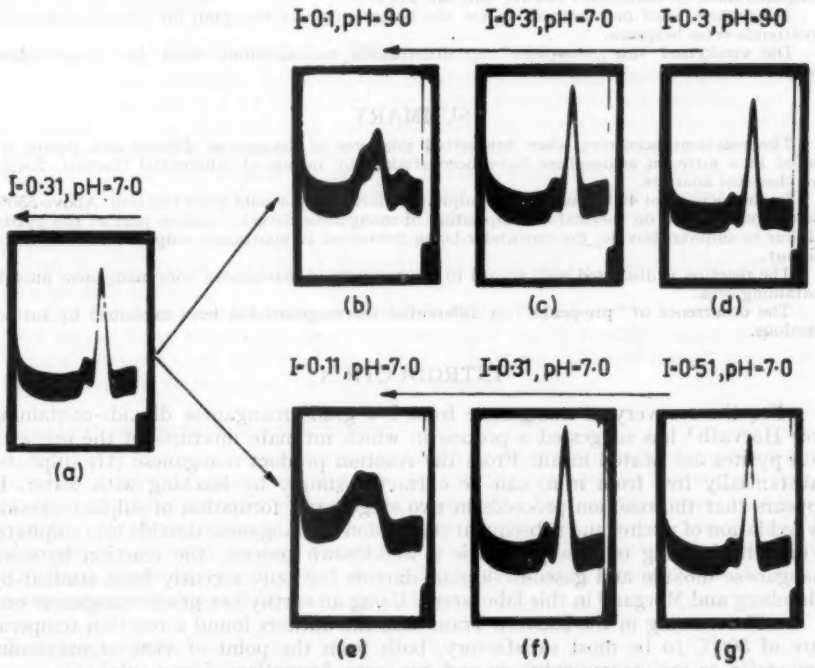

Fig. 5. Sedimentation diagrams of Fraction B in different buffers.

This paper is published with the permission of the South African Council for Scientific and Industrial Research.

National Chemical Research Laboratory,
Council for Scientific and Industrial Research,
Pretoria.

Received, July 4, 1955.

REFERENCES

[1] Osborne, T. B. and Campbell, G. F., *J. Amer. Chem. Soc.*, 1898, **20**, 348.
[2] Danielsson, C. E., *Biochem. J.*, 1949, **44**, 387.

ON THE REACTION BETWEEN MANGANESE DIOXIDE AND IRON PYRITES

by

R. A. W. HAUL and H. J. SCHUMANN

OPSOMMING

Die reaksies wat plaasvind wanneer saamgeperste mengsels van mangaandioksied en ysterpiriet in 'n stikstofatmosfeer verhit word is deur middel van differensiëel-termiese, röntgenografiese en chemiese analise bestudeer.

In die omgewing van 400°C word mangaansulfaat deur 'n vaste-toestandsreaksie gevorm. Bokant 550°C okisdeer die suurstof wat by die termiese ontbinding van mangaandioksied afgegee word, 'n gedeelte van die piriet-swawel na swaweldioksied, terwyl die oorblywende swawel na mangaansulfied en elementêre swawel omgesit word.

Die reaksie word met betrekking tot die herwinning van mangaan uit mangaan-dioksiedbevattende ertse bespreek.

Die verskynsel van „voorpieke" op differensiële termogramme word deur oppervlaktereaksies verklaar.

SUMMARY

The reactions occurring when briquetted mixtures of manganese dioxide and pyrite are heated in a nitrogen atmosphere have been studied by means of differential thermal, X-ray, and chemical analysis.

In the vicinity of 400°C manganese sulphate is formed by a solid state reaction. Above 550°C the oxygen evolved on thermal decomposition of manganese dioxide oxidises part of the pyritic sulphur to sulphur dioxide, the remainder being converted to manganese sulphide and elemental sulphur.

The reaction is discussed with regard to the recovery of manganese from manganese dioxide containing ores.

The occurrence of "pre-peaks" on differential thermograms has been explained by surface reactions.

INTRODUCTION

For the recovery of manganese from low grade manganese dioxide-containing ores Horvath [1] has suggested a process in which intimate mixtures of the ore with iron pyrites are heated in air. From the reaction product manganese (II) sulphate, substantially free from iron, can be extracted simply by leaching with water. It appears that the reaction proceeds in two stages, viz. formation of sulphur dioxide by oxidation of pyrite, and subsequent conversion of manganese dioxide into sulphate. While the burning of iron pyrites is a well-known process, the reaction between manganese dioxide and gaseous sulphur dioxide has only recently been studied by Blumberg and Morgan [2] in this laboratory. Using an earthy low-grade manganese ore, a "wad" occurring in the Eastern Transvaal, the authors found a reaction temperature of 300°C to be most satisfactory, both from the point of view of maximum conversion to manganese sulphate and minimum formation of iron sulphate.

The roasting of mixtures of iron pyrites and manganese dioxide has recently been studied further by Moorthy and Datar [3]. With a view to reducing the losses of sulphur, the authors investigated a process in which the mixtures were first heated at about 500°C in the absence of air, with subsequent oxidation of the intermediate reaction products at about 300°C. A study of the reaction mechanism appeared to be of interest, particularly as it was considered probably that a solid state reaction might be involved in this process. For this purpose, briquetted mixtures of pyrite and manganese dioxide were heated in oxygen-free nitrogen under various conditions and the reaction products studied by means of differential thermal, X-ray and chemical analysis.

EXPERIMENTAL

Materials

Well crystallised pyrite which contained only small amounts of quartz was used. The mineral was crushed and the quartz crystals removed by hand. After further grinding, during which care was taken to prevent oxidation, the material was screened and the fraction passing through a 325-mesh sieve used for the experiments. Chemical analysis gave 51·7 *per cent.* sulphur (theor. 53·5) and 46·1 *per cent.* iron (theor. 46·6), corresponding to a composition $FeS_{1.95}$.

From a pyrolusite ore (Rietpan, Lichtenburg, Transvaal) well developed crystals were selected, finely ground and passed through a 325-mesh sieve. On the basis of available oxygen the MnO_2 content was 92·6 *per cent.* In addition, manganese dioxide BDH Laboratory Reagent, was used in some experiments.

Intimate mixtures of pyrite and manganese dioxide in the molar ratios 2:1, 1:1, and 1:2 were compressed in a steel holder to give firm tablets of 1 cm diameter and 0·4 cm thickness.

Differential thermal analysis (DTA)

The DTA apparatus in use in this laboratory has been described by Theron[4]. Since the analysis had to be carried out under a controlled atmosphere, the same technique was applied as in a previous study on the thermal decomposition of dolomite[5]. After the reaction vessel had been flushed out with oxygen-free nitrogen[6], the gas stream was turned off and the heating started during which any excess pressure could escape through a sulphuric acid trap. In order to prevent damage by reaction with metal oxides and/or sulphides, the thermocouple junctions were protected by thin-walled quartz tubes. These were inserted into small holes carefully drilled in the sample tablets. A tight fit was obtained by compressing some loose powder into any gaps.

The reference material was also used in tablet form in order to esnure the same heat conductivity conditions. Since alumina could not be readily compressed, kaolin tablets were prepared and fired at 1,200°C before use. The α-β quartz inversion at 573°C served to standardise the temperature scale.

Constant temperature experiments

When it had been found by means of DTA at what temperatures reactions occur, these were further studied individually by heating the samples for various lengths of time at the particular temperatures indicated. The samples were placed in a quartz tube through which a slow stream of oxygen-free nitrogen was passed. The exit gas was bubbled through two traps containing sodium hydroxide. After all air had been displaced, the tube was inserted into a furnace already set at the desired temperature which could be controlled within $\pm$ 5°C.

X-ray analysis

X-Ray powder photographs were taken with the Norelco Philips High Angle Goniometer, iron-Kα and cobalt-Kα radiation being used. Identification of the diagrams was achieved by the use of the ASTM X-ray diffraction data[7].

Chemical analysis

Apart from anlysis of the raw materials, only a few orientative analyses were carried out, viz. determination of water soluble sulphate in the reaction products and sulphur dioxide in the exit gas. The reacted samples were extracted with cold water and sulphate was determined gravimetrically as barium sulphate. The sulphur dioxide was absorbed in sodium hydroxide, the resulting sulphite oxidised to sulphate with hydrogen peroxide and the latter determined gravimetrically.

RESULTS AND DISCUSSION

I. Differential thermal analysis

The thermograms of the raw materials are shown in Fig. 1 and will be discussed first.

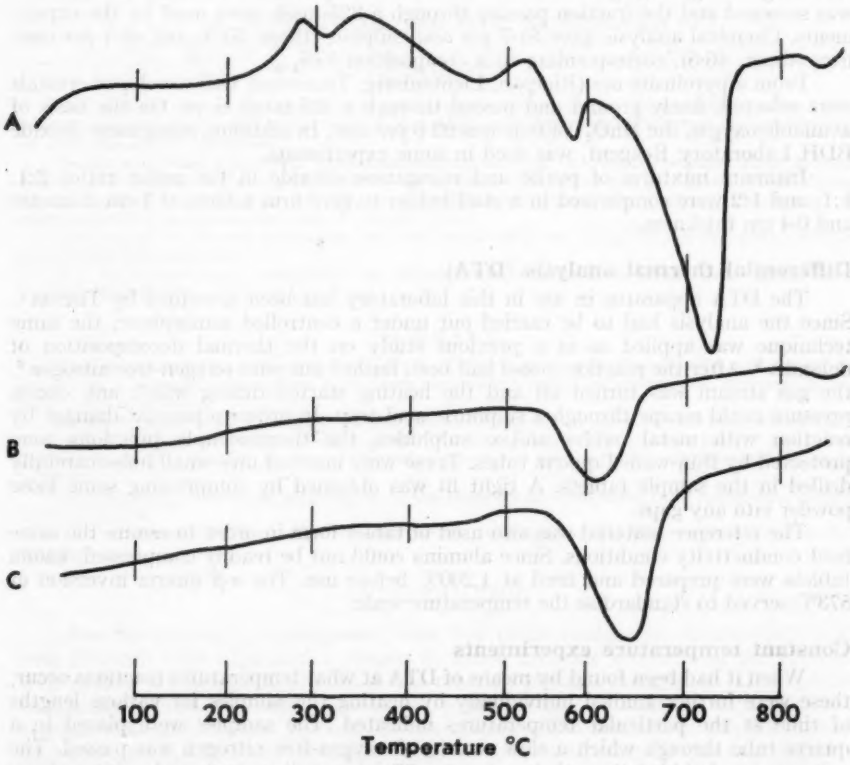

Fig. 1.

Thermograms of (A) pyrite, (B) BDH manganese dioxide, and (C) pyrolusite. Heating in a nitrogen atmosphere.

Iron pyrites. On heating pyrite in a nitrogen atmosphere the following reactions are indicated: two exothermic at 270 and 340°C, and three endothermic at 580, 730 and 830°C. In order to investigate the nature of these reactions, pyrite samples were heated at the various temperatures for one hour and the reaction products examined by X-ray analysis. From Fig 2 A and B it can be seen that the diagram of the product obtained at 450°C is almost identical with that of the original pyrite; the same is true for a sample heated at 270°C. Slight variations in intensities are probably due to different packing of the samples. Thus X-ray analysis does not provide an explanation for the two exothermic peaks, the origin of which was not further studied.

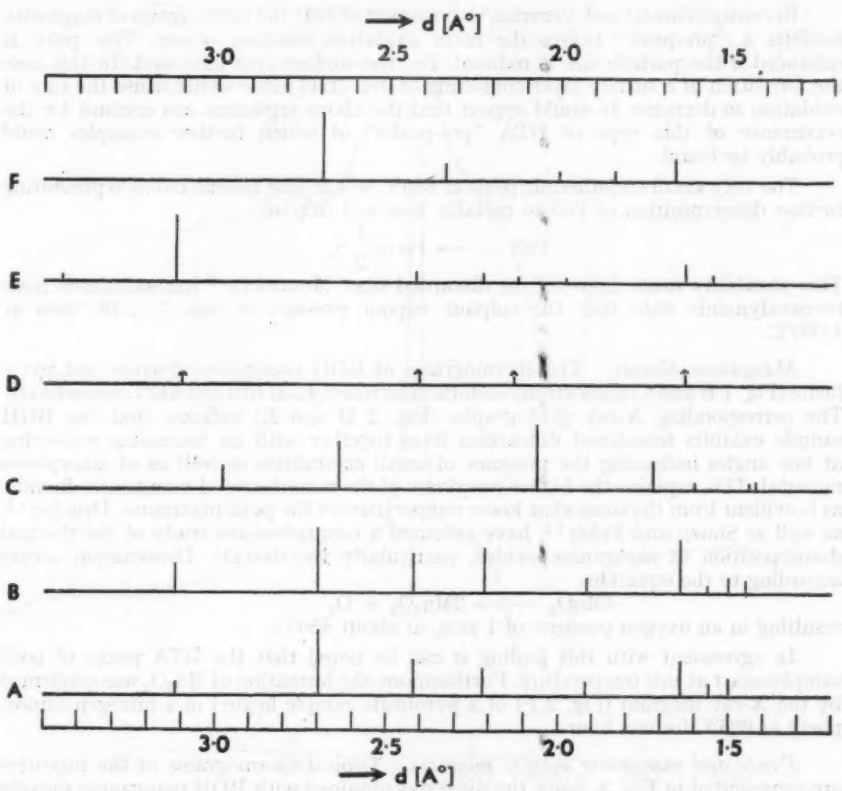

Fig. 2.
X-Ray powder diagrams of the raw materials and their reaction products obtained on heating in nitrogen. (A) pyrite, (B) and (C) pyrite heated at 450 and 700°C for one hour respectively, (D) BDH MnO_2, (E) pyrolusite, (F) pyrolusite heated at 625°C for one hour. Intensities relative to the strongest line in each diagram.

Pyrite heated at 700°C results in a diagram (Fig. 2 C) in which the FeS_2 pattern has disappeared completely, FeS appearing as the only reaction product.

$$FeS_2 \longrightarrow FeS + \frac{1}{2} S_2$$

This reaction has been studied by Juza, Biltz and Meisel[8] who found that the sulphur vapour pressure becomes appreciable above 600°C. The thermogram is in agreement with this finding, but shows an additional interesting feature, viz. a small peak at 580°C preceding the main endothermic reaction at 730°C. The following explanation for the occurrence of this "pre-peak" is suggested. Decomposition starts already at the lower temperature at the surface of the individual crystals and the resulting layer of FeS hinders further decomposition which would have to occur by a lattice diffusion process. At higher temperatures the layer breaks up into crystallites permitting the sulphur to escape through intergranular channels. The bulk of the pyrite crystals then decomposes, giving rise to the strong endothermic peak.

Recently Schmidt and Vermaas[9] have reported that the thermogram of magnetite exhibits a "pre-peak" before the main oxidation reaction occurs. This peak is enhanced if the particle size is reduced, i.e., the surface area increased. In this case the formation of a surface layer consisting of iron (III) oxide would cause the rate of oxidation to decrease. It would appear that the above argument can account for the occurrence of this type of DTA "pre-peaks" of which further examples could probably be found.

The very small endothermic peak at 830°C was at first considered as representing further decomposition of FeS to metallic iron and sulphur.

$$FeS \longrightarrow Fe + \frac{1}{2} S_2$$

This possibility must, however, be discarded since Morawietz[10] has calculated from thermodynamic data that the sulphur vapour pressure is only 7×10^{-5} mm at 1,000°C.

Manganese dioxide. The thermograms of BDH manganese dioxide and pyrolusite (Fig. 1 B and C) show strong endothermic reactions at 610 and 630°C respectively. The corresponding X-ray photographs (Fig. 2 D and E) indicate that the BDH sample exhibits broadened diffraction lines together with an increasing scattering at low angles indicating the presence of small crystallites as well as of amorphous material. This explains the higher reactivity of the manufactured manganese dioxide, as is evident from the somewhat lower temperature of the peak maximum. Drucker[11], as well as Simon and Fehér[12], have executed a comprehensive study of the thermal decomposition of manganese oxides, particularly the dioxide. Dissociation occurs according to the equation

$$4MnO_2 \longrightarrow 2Mn_2O_3 + O_2$$

resulting in an oxygen pressure of 1 atm. at about 550°C.

In agreement with this finding it can be noted that the DTA peaks of both samples start at this temperature. Furthermore, the formation of Mn_2O_3 was confirmed by the X-ray diagram (Fig. 2 F) of a pyrolusite sample heated in a nitrogen atmosphere at 625°C for one hour.

Pyrite and manganese dioxide mixtures. Typical thermograms of the mixtures are represented in Fig. 3. Since the diagrams obtained with BDH manganese dioxide and pyrolusite are practically the same, only those of mixtures with the latter are shown. For a 1:1 molar ratio of pyrite and pyrolusite, three exothermic reactions are indicated at 270, 360 and 420°C, followed by a strong endothermic reaction at about 600°C and a further very small peak at 830°C. The thermogram for a 1:2 molar mixture (Fig. 3 B) is similar, the only difference being that the first two peaks merge and that the peak at about 420°C is notably enhanced.

Whereas the first two exothermic reactions are also indicated on the thermogram of pyrite itself, the peak at 420°C is not exhibited by the raw materials. The fact that this reaction occurs far below the decomposition temperature of either pyrite or manganese dioxide provides strong evidence that a solid state reaction proceeds under these circumstances.

The reaction at about 600°C occurs just below the temperature of the peak maximum for pyrolusite. It would therefore appear that this reaction is associated with the thermal decomposition of manganese dioxide into a lower oxide and oxygen.

The small endothermic peak at 830°C is exhibited by pyrite, the BDH manganese dioxide, as well as by all the mixtures used. Thus the peak appears to have no bearing on the reaction under investigation and may be inherent in the experimental arrangements. Possibly a reaction could occur between the heavy metal oxides and the quartz sample and/or thermocouple holders at this temperature.

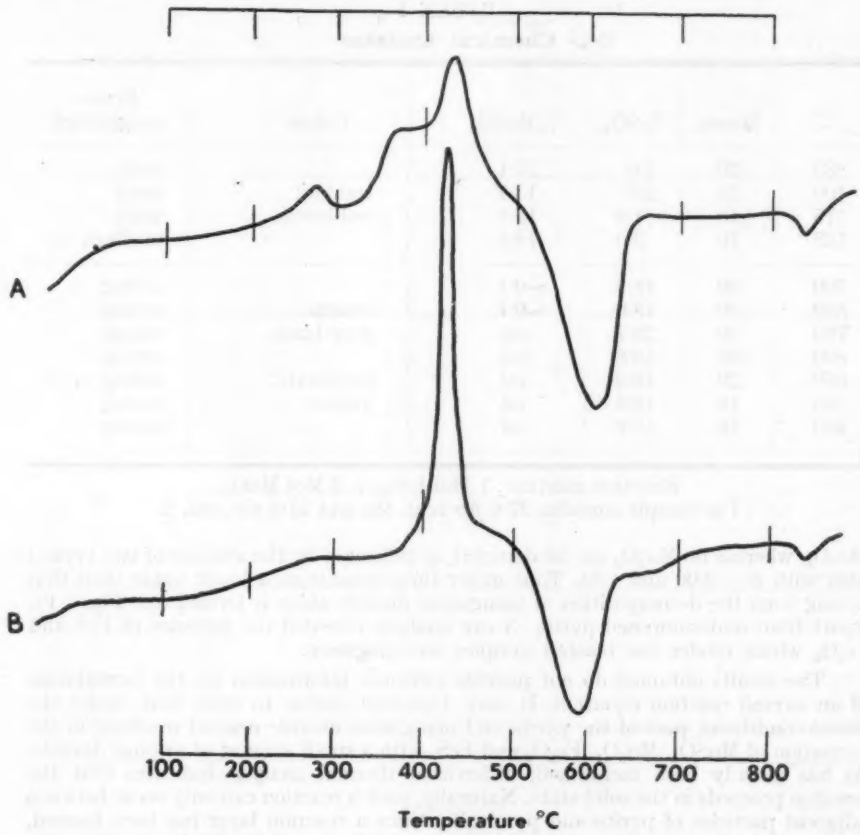

Fig. 3.
Thermograms of pyrite and pyrolusite mixtures: (A) 1 Mol FeS_2 + 1 Mol MnO_2 (B) 1 Mol FeS_2 + 2 Mol MnO_2.

Summarising the DTA results, it follows that two distinctly different reactions occur at 400°C and 600°C respectively. These were further studied on a 1:2 molar mixture of pyrite and pyrolusite using the techniques already described.

II. 400°C-Reaction

A number of experiments was carried out in the vicinity of this temperature, viz. at 380, 400, 415 and 425°C. From chemical analysis of the products (Table I) it is apparent that water soluble manganese sulphate was formed under these conditions. No iron could be detected colorimetrically in the aqueous extract. Unfortunately, the X-ray diffraction lines of possible reaction products overlap to such an extent that no line can be attributed solely to manganese sulphate, although all lines of this compound can be accounted for. This coincidence of diffraction lines (Fig. 4 B) rendered the identification of further reaction products difficult. The following conclusions can, however, be drawn. Part of the manganese dioxide is converted to

TABLE I

Chemical Analyses

°C	Hours	$\%SO_2$	$\%MnSO_4$	Colour	Ferro-magnetism
380	20	2·0	11·1		weak
400	20	2·3	13·7	residue:	weak
415	10	1·8	15·1	red-brown	weak
425	10	3·0	14·1		medium
500	20	15·5	~0·1		strong
550	20	18·0	~0·1	residue:	strong
750	20	20·7	nil	grey-black	strong
800	20	18·8	nil		strong
850	20	18·9	nil	sublimate:	strong
900	10	18·8	nil	yellow	strong
950	10	15·7	nil		strong

Reaction mixture: 1 Mol FeS_2 + 2 Mol MnO_2.
The sample contains 37·6 *per cent.* Mn and 21·4 *per cent.* S.

Mn_3O_4, whereas no Mn_2O_3 can be detected, as indicated by the absence of two typical lines with d = 2·00 and 1·84. Thus under these conditions a lower oxide than that arising from the decomposition of manganese dioxide alone is formed (see Fig. 2 F). Apart from undecomposed pyrite, X-ray analysis revealed the presence of FeS and Fe_3O_4 which render the reacted samples ferromagnetic.

The results obtained do not provide sufficient information for the formulation of an overall reaction equation. It may, therefore, suffice to state that, under the above conditions, part of the pyrite and manganese dioxide reacted resulting in the formation of $MnSO_4$, Mn_3O_4, Fe_3O_4 and FeS, with a small amount of sulphur dioxide. As has already been mentioned, differential thermal analysis indicates that the reaction proceeds in the solid state. Naturally, such a reaction can only occur between adjacent particles of pyrite and pyrolusite. Once a reaction layer has been formed, further reaction can only proceed by means of diffusion of the lattice constituents. Consequently, the reaction rate decreases with increasing thickness of the reaction layer. Since at 400°C rates of diffusion in solids such as those under investigation are still low, the reaction does not go to completion even after reaction periods of 20 hours. Further experimentation would be required to elucidate the mechanism of this solid state reaction with regard to the nature of the diffusing constituents.

III. 600°C-Reaction

In the temperature range 500 to 550°C the mechanism of the reaction changes profoundly. The X-ray diagram of a mixture which had been heated at 550°C for 20 hours illustrates this point (Fig. 4 C). The raw materials, pyrite and pyrolusite, have completely disappeared and no manganese sulphate is detectable. This is also supported by chemical analysis (Table I) which shows that less than 0·1 *per cent.* water soluble sulphate was present in the reaction product . On the other hand, sulphur-dioxide was now a major reaction product. Some elemental sulphur was also formed and deposited as a yellow sublimate on the cooler parts of the reaction vessel. The main solid reaction product was Fe_3O_4, whereas the formation of Mn_3O_4 had decreased, as is indicated by the d = 2·76 diffraction line which has dropped to a very low

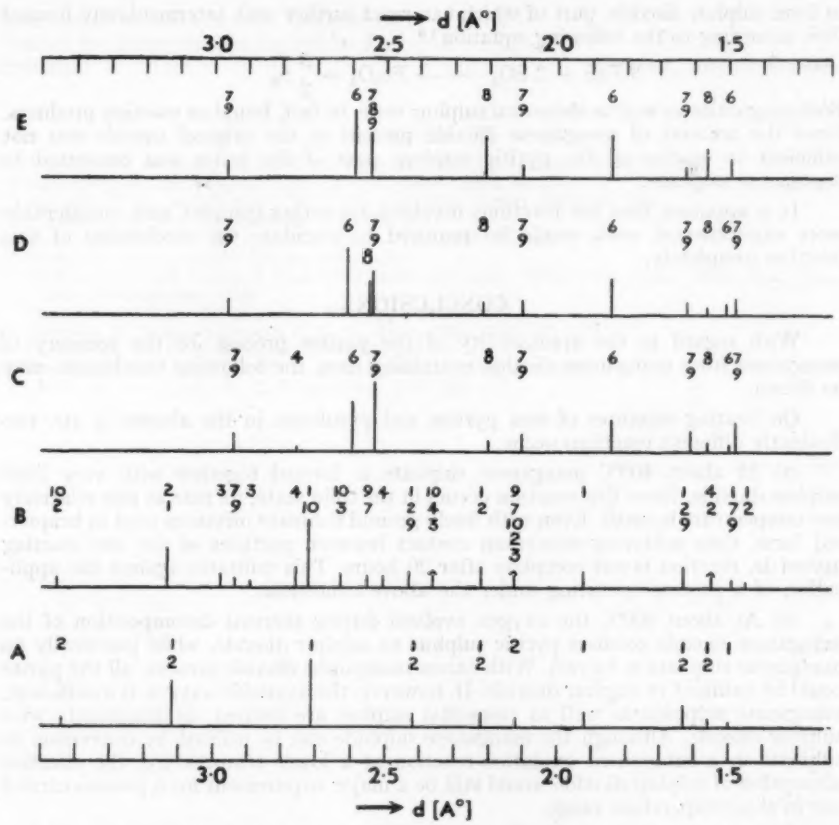

Fig. 4.

X-Ray powder diagrams of reaction products. Mixture of 1 Mol FeS_2 + 2 Mol MnO_2 (A) original mixture, (B) heated at 415°C for 10 hours, (C) ditto at 550°C, for 20 hours, (D) ditto at 595°C, 20 hours, (E) ditto at 950°C, 10 hours.
1 = FeS_2, 2 = MnO_2, 3 = FeS, 4 = Mn_3O_4, 5 = Mn_2O_3, 6 = MnS, 7 = Fe_3O_4, 8 = MnO, 9 = $(Fe,Mn)Fe_2O_4$, 10 = $MnSO_4$.

intensity (Fig. 4 C). This may be due to the formation of the spinel jacobsite (Fe, Mn)Fe_2O_4, although X-ray data do not permit a simple distinction between this compound and magnetite. Manganese dioxide was converted to MnO and MnS, the latter being present as the α-modification (NaCl-type). No FeS and FeO could be detected.

At higher reaction temperatures, up to 950°C, the same reaction products were found as is evident from the X-ray diagrams in Fig. 4 D and E.

The DTA results indicated that the mechanism changes from a solid state to a gas-solid type reaction when the oxygen dissociation pressure of manganese dioxide becomes appreciable above 550°C. The oxygen evolved then reacts with the pyrite

to form sulphur dioxide, part of which can react further with intermediately formed FeS, according to the following equation[10]

$$3\ FeS + 2\ SO_2 \longrightarrow Fe_3O_4 + \frac{5}{2}\ S_2$$

Both magnetite as well as elemental sulphur were, in fact, found as reaction products. Since the amount of manganese dioxide present in the original sample was not sufficient to oxidise all the pyritic sulphur, part of the latter was converted to manganese sulphide.

It is apparent that the reactions involved are rather complex and considerably more experimental work would be required to elucidate the mechanism of this reaction completely.

CONCLUSIONS

With regard to the applicability of the pyrites process for the recovery of manganese from manganese dioxide containing ores, the following conclusions may be drawn.

On heating mixtures of iron pyrites and pyrolusite in the *absence of air*, two distinctly different reactions occur.

(a) At about 400°C manganese sulphate is formed together with very little sulphur dioxide. Since this reaction occurs in the solid state, its rate at this relatively low temperature is small. Even with finely ground intimate mixtures used in briquetted form, thus achieving maximum contact between particles of the two starting materials, reaction is not complete after 20 hours. This militates against the application of a process operating under the above conditions.

(b) At about 600°C the oxygen evolved during thermal decomposition of the manganese dioxide oxidises pyritic sulphur to sulphur dioxide, while practically no manganese sulphate is formed. With excess manganese dioxide present, all the pyrite could be oxidised to sulphur dioxide. If, however, the available oxygen is insufficient, manganese sulphide as well as elemental sulphur are formed simultaneously with sulphur dioxide. Although the manganese sulphide can be utilised by conversion to sulphate in a subsequent oxidation-reaction at a lower temperature, the effective absorption of sulphur dioxide would still be a major requirement for a process carried out in this temperature range.

Summarising, it would appear that a reaction in which the mixture of iron pyrites and pyrolusite is first heated in the absence of air does not offer attractive practical possibilities. The importance of the presence of an oxygen atmosphere during roasting is clearly stressed by the following overall equation

$$4\ MnO_2 + FeS_2 + \frac{11}{2}\ O_2 \longrightarrow 4MnSO_4 + Fe_2O_3$$

Chemically, this reaction is straightforward, but the design of a feasible technical process remains as an engineering problem. In such a process it would be required to introduce the necessary oxygen in a suitable way and to achieve an effective absorption of the intermediately formed sulphur dioxide by unreacted manganese dioxide. It would largely depend on these requirements whether roasting of a mixture of the raw materials is more advantageous than separate burning of iron pyrites and subsequent reaction of the sulphur dioxide with manganese ore. Naturally, the availability of iron pyrites would be a determining factor for any economic industrial application of the above reaction.

This paper is published with the permission of the South African Council for Scientific and Industrial Research.

National Chemical Research Laboratory,
Council for Scientific and Industrial Research,
Pretoria.

Received, August 3, 1955.

REFERENCES

[1] Horvath, Z., *Bányász. kohász. Lap.*, 1949, **82**, 202; *Chem. Abstr.*, 1951, **45**, 994.
[2] Blumberg, R. and Morgan, T. D., *J. appl. Chem.*, 1953, **3**, 223.
[3] Moorthy, K. N. and Datar, D. S., *J. Sci. ind. Res.* (India), 1951, **10**, 196.
[4] Theron, J. J., *Rev. Sci. Instrum.*, 1953, **24**, 281.
[5] Haul, R. A. W. and Heystek, H., *Amer. Min.*, 1952, **37**, 166.
[6] McArthur, I. A., *J. appl. Chem.*, 1952, **2**, 91.
[7] Alphabetical and Grouped Numerical Index of X-ray Diffraction Data. Amer. Soc. Test. Mat. Philadelphia, 1950.
[8] Juza, R. and Biltz, W., *Z., anorg. Chem.*, 1932, **205**, 273.
[9] Schmidt, E. R. and Vermaas, F. H. S., *Amer. Min*, 1955, **40**, 422.
[10] Morawietz, W., *Z. Elektrochem.*, 1953, **57**, 539.
[11] Drucker, C. and Huettner, R. *Z. phys. Chem.* (A) 1928, **131**, 237.
[12] Simon, A. and Fehér, F., *Z. Elektrochem.*, 1932, **38**, 137.

CHEMISORPTION STUDIES ON SOME FISCHER-TROPSCH IRON CATALYSTS

by

F. A. RAAL

OPSOMMING

Chemiesorpsie van koolstofmonoksied, koolstofdioksied en waterstof op sekere presipiteerde en sintetiese-ammoniak-tipe kataliste is bestudeer.

Die metode van lae-temperatuur-chemiesorpsie van koolstofmonoksied vir die bepaling van die „vry-yster-oppervlakte" van 'n katalis is uitgetoets.

Adsorpsie van waterstof en koolstofmonoksied is as 'n funksie van die temperatuur tot by sintese-temperature ondersoek. Snelhede van chemiesorpsie is in die temperatuurgebied 140°C —180°C bepaal en die resultate word aan die hand van bestaande snelheidsvergelykings bespreek.

SUMMARY

Chemisorption of carbon monoxide, carbon dioxide and hydrogen on some precipitated and synthetic-ammonia-type catalysts has been studied.

The method of assessing the "free iron surface" on a catalyst by means of low temperature chemisorption of carbon monoxide has been tested.

Adsorption of hydrogen and carbon monoxide, as a function of temperature, has been followed up to synthesis temperatures.

Rates of chemisorption of carbon monoxide have been measured in the temperature range 140°C — 180°C and the results are discussed in the light of existing rate equations .

INTRODUCTION

In heterogeneous catalysis adsorption of the reacting molecules by the catalyst is the initial step and it is, for this reason, that adsorption studies are of fundamental significance in any endeavour to throw light on the mechanism of catalytic processes.

Two main types of adsorption are to be clearly distinguished, namely, physical adsorption and chemisorption. In physical adsorption the adsorbed molecules are held to the surface of the adsorbent by van der Waal's forces and the heat evolved during adsorption is of the order of the heat of liquefaction of the adsorbate. Physical adsorption is usually rapid and reversible.

In chemisorption, the adsorbed molecules are held to the surface by valence forces of the same nature as those encountered in the formation of molecules. These forces are much stronger than van der Waal's forces and the heats evolved during chemisorption are of the same order as those liberated in chemical reactions. In most cases chemisorption is irreversible since the electronic structure of the molecule is profoundly altered on adsorption. The rate of chemisorption varies from very rapid to extremely slow. In the case of clean metal surfaces, e.g. freshly formed films, chemisorption is practically instantaneous. In bulk catalysts, however, where the surface is usually covered by a layer of adsorbed molecules, the rate of chemisorption is strongly dependent on temperature thus involving an activation energy.

Since both reactants carbon monoxide and hydrogen are chemisorbed on the catalyst in the Fischer-Tropsch synthesis, a creditable amount of work has been done in this connection especially with a view to the postulation of a reaction mechanism. Although quite a few theories have been advanced we are, as yet, far from a satisfactory explanation of what really happens during synthesis. One of the results that emerged from these studies, however, is a method developed by Emmett and Brunauer [1] to assess the available "free iron surface" of a catalyst or, alternatively, to determine the fraction of the surface of an iron catalyst covered by such promoters as potassium oxide and/or aluminium oxide. This is done by comparing the low

temperature chemisorption of carbon monoxide on the catalyst with the total surface area as measured by nitrogen adsorption. In most of the catalysts investigated by the above authors chemisorption of carbon monoxide was in the region of 50 *per cent.* as compared with the nitrogen monolayer. In the case of pure iron, as shall be pointed out, the effect was inexplicably much smaller. In our initial experiments along these lines surprisingly small values for the chemisorption of carbon monoxide on the catalysts were evident, and it was therefore deemed expedient to explore this matter further.

Adsorption isobars have yielded some of the more interesting information about chemisorption processes. With the aid of isobars the effect of temperature on adsorption can be investigated and it has been shown that different types of adsorption can occur on one and the same catalyst, probably on different parts of the surface[2]. The low temperature adsorption mentioned above was therefore extended to cover temperatures in the region of actual synthesis.

In conclusion work on the rate of adsorption of carbon monoxide by some of the catalysts is described. The scope of this investigation was limited, however, because of experimental inadequacy as well as the fact that the process of adsorption was a complex one involving, also, diffusion within the pores of the catalysts.

EXPERIMENTAL

Materials

The investigation described in this paper was carried out with fused synthetic-ammonia-type catalysts and partly reduced, precipitated catalysts The former, designated by the letters A and B, were prepared by electrical fusion of magnetite and mill scale, respectively, followed by reduction in the units from which the samples were drawn. Since the precipitated catalysts C and D were pyrophoric, great care was exercised throughout in the handling and sampling of these catalysts which were stored under heptane. Samples for our experiments were taken from the bulk catalyst in a carbon dioxide atmosphere to the exclusion of all air which had a deleterious effect on the catalysts.

Chemical analyses of the catalysts yielded the following information about the various chemical and/or structural promoters in which we are primarily interested.

TABLE I*

Percentage composition of catalysts.

Component	*A*	*B*	*C*	*D*
Free iron	—	—	17·9	14·6
Silicon dioxide	1·14	0·28	~18	~15
Aluminium oxide	0·87	0·48	traces	0·14
Titanium dioxide	0·19	traces		
Potassium oxide	0·62	0·38	2·58	2·38
Magnesium oxide	0·20	0·48	0·11	0·06
Calcium oxide			6·10	0·22
Copper	traces	traces	2·36	0·22

Carbon monoxide was prepared from a mixture of formic and sulphuric acids and carbon dioxide by heating analar sodium bicarbonate. The gases were dried and

* Analyst, Mr. F. W. E. Strelow, National Chemical Research Laboratory.

purified in the usual manner. The purity was checked in each instance by determining the vapour pressure at a known temperature. Helium and argon of high purity were obtained from the Matheson Co. Inc. Hydrogen and nitrogen were of local commercial manufacture and were freed from oxygen and water vapour by passage over hot reduced copper and through anhydrous magnesium perchlorate. In one experiment specially pure hydrogen needed to be used. This was prepared from carefully degassed distilled water by reaction with amalgamated aluminium foil which, also, had been thoroughly evacuated. Prior to use, the hydrogen was passed through a silica gel trap coolled to −183°C.

Apparatus and procedure

The apparatus used was the conventional volumetric adsorption one[3]. Adsorption isotherms and rates of adsorption were determined in the usual manner from the volumes of adsorbate admitted from time to time. Appropriate corrections were applied for the "dead space" and the non-ideality of the adsorbed gases.

For maintaining the catalyst under investigation at constant temperatures below 0°C, use was made of various constant temperature baths. For higher temperatures an electric tube furnace was employed. By means of an electronic device the temperature could be controlled automatically to within $\pm$ 1·5°C at 300°C.

At low temperatures equilibrium was established rather rapidly in all cases. At the elevated temperatures, however, equilibrium was slow and indefinite and, in the case of carbon monoxide adsorption, a slow but definite adsorption was still evident at 200°C even after 72 hours. In view of this fact adsorption readings were taken at regular intervals of 60 minutes and the measurements so obtained regarded as representative of the true equilibrium state.

As a rule, the catalysts were used as such and only subjected to prolonged outgassing at 300°C before each measurement. This temperature was chosen since it was found that higher temperatures caused slight sintering with a corresponding change in the surface area and sorptive properties of the catalysts. In some cases reduction of the catalysts by hydrogen was necessary. This reduction was carried out with pure, dry hydrogen at 300°C for some 15 hours and the catalyst subsequently outgassed. The procedure of outgassing adopted, in general, was to pump the catalyst under investigation to a hard vacuum at approximately 100°C for 2 hours followed by evacuation for a further 3 — 8 hours at 300°C. This was done before each separate determination. It is realised that this method of outgassing does not suffice to render the surface free from all contaminants, but this cannot be avoided when working with bulk catalysts at as low a temperature as 300°C. Repeat experiments indicated that the above treatment invariably gave good reproducibility.

SURFACE AREAS AND PORE CHARACTERISTICS

Surface areas were determined from the nitrogen adsorption isotherms at liquid oxygen temperature. These are given in Table II and were obtained from B.E.T. monolayer capacities (V_m) taking the cross-sectional area of the adsorbed nitrogen molecule as 17 Å^2.

The average pore sizes of the precipitated catalysts C and D were obtained from the argon adsorption isotherms at −183°C taken up to high relative pressures. On desorption hysteresis was observed in both instances and the average pore sizes were calculated by means of the Kelvin equation from the steepest parts of the desorption branches of the isotherms. The adsorption method for determining porosities was not applicable to the fused catalysts and pore diameters (d) were calculated from the equation $d = \frac{4V}{S}$, where V = pore volume and S = surface area.

The pore volume was evaluated as the difference of the reciprocals of the mercury and helium densities. The results are summarised in Table II.

TABLE II

Surface areas and porosities of catalysts.

Catalyst	*C (B.E.T.)*	V_m *cc/g N.T.P.*	*Surface area sq. m/g N.T.P.*	*Density*		*Pore volume cc/g*	*Pore diameter* Å
				Hg g/cc	*He g/cc*		
A	89	1·61	7·4	3·97	6·64	0·101	550
B	113	1·50	6·9	2·81	6·44	0·201	1150
C	112	47·0	216	—	—	—	190
D	95	39·5	182	—	—	—	• 120

RESULTS AND DISCUSSIONS

1. Low temperature chemisorption of carbon monoxide and carbon dioxide.

In these experiments we shall only compare catalysists A and C as representatives of the two types of catalysts and mention B and D where relevant.

Adsorption isotherms for the adsorption of nitrogen, carbon monoxide and carbon dioxide by catalysts A and C are presented in Figures 1 and 2 respectively. A cursory inspection of the carbon dioxide isotherms shows that the total carbon dioxide adsorption at −80°C as compared to the corresponding adsorption of nitrogen at −183°C varies markedly in the cases of the two catalysts. With catalyst C the total carbon dioxide adsorption at −80°C is of the same order as the nitrogen adsorption at −183°C while, on the same basis, the total carbon dioxide adsorption is appreciably more as regards catalyst A. A reasonable explanation of the excess of carbon dioxide taken up by A is the one put forward by Emmett and Brunauer[1] whereby it is assumed that the catalyst, by virtue of its alkali content, has the property of chemisorbing carbon dioxide over and above the normal amount of physical adsorption.

In order to ascertain whether chemisorption of carbon dioxide was actually occurring, the method of Emmett and Brunauer was adopted. After the total carbon dioxide adsorption had been determined at −80°C, the catalyst was evacuated by a mercury diffusion pump at 20°C, i.e., approximately 100°C above the temperature of adsorption for 30 minutes. A carbon dioxide isotherm at −80°C immediately following this evacuation gave the amount of physically adsorbed carbon dioxide. The difference between the total carbon dioxide and the van der Waal's carbon dioxide was then taken as the amount of chemisorbed carbon dioxide.

In this way it was established that catalyst A with a nitrogen monolayer, V_m, of 1·61 cc N.T.P./g exhibited carbon dioxide chemisorption to the extent of 0·48 cc N.T.P./g. This gives a value of 0·30 for the ratio V_{CO_2}/V_m and implies that a considerable portion of the surface of A is covered by chemisorbed carbon dioxide. This result is noteworthy since the potassium oxide content of the catalyst is rather small (0·62%). Emmett and co-workers took this as strong evidence of the enrichment of potassium or potassium compounds in the surface of the catalyst.

In the case of catalyst C the two carbon dioxide isotherms virtually coincide, indicating that chemisorption is absent, even though the potassium oxide content is fairly high. The most probable explanation of the absence of chemisorption, in this particular case, is the presence of a high silica content which is capable of binding the potassium within the bulk of the material. In the synthetic-ammonia-type catalyst, on the other hand, due to the immiscibility of the iron and potassium oxide, the latter compound is precipitated on the surface.

Chemisorption of carbon monoxide at liquid oxygen temperature was investigated in the same way. The total carbon monoxide adsorption at −183°C was first determined, followed by the physically adsorbed carbon monoxide at the same temperature after evacuation for 30 minutes at −80°C. The difference between the two isotherms constituted the chemisorbed carbon monoxide which could then be expressed as a percentage in terms of the nitrogen monolayer V_m. The results are tabulated in Table III.

TABLE III

Percentage chemisorption of carbon monoxide by catalysts.

Catalyst	$V_m(N_2)$ cc N.T.P./g	V_{CO} cc N.T.P./g	V_{CO}/V_m per cent.
A	1·61	0·24	14·9
B	1·50	0·22	14·7
C	47·0	0	0
D	39·5	1·0	2·5

For some time now chemisorption of carbon monoxide has been regarded as a method of assessing the available "free iron surface" of a catalyst by virtue of the fact that carbon monoxide is bound by the iron atoms. Alternatively, chemisorption of carbon dioxide is a measure of the fraction of an iron catalyst covered by such promoters as potassium and/or aluminium oxide. Thus, it was shown by Emmett and his collaborators that the higher the carbon dioxide chemisorption, the lower the carbon monoxide chemisorption thereby revealing the relevant fractions occupied by potassium and iron.

The chemisorption of carbon monoxide found for both fused catalysts (see Table III), as well as the chemisorption of carbon dioxide as observed with catalyst A, are in agreement with the findings of Emmett and his school on synthetic-ammonia-type catalysts. The amount of chemisorbed carbon monoxide is, however, appreciably smaller than that reported in the literature for similar catalysts. In Emmett's experiments the catalysts were reduced and subsequently outgassed at 500°C instead of 300°C as in the present experiments. This can have a pronounced effect on the surface since it is known that at 500°C, even after 24 hours evacuation, as much as 15 — 20 *per cent.* of the iron surface of a promoted iron catalyst may be covered by chemisorbed hydrogen [4]. Furthermore, contamination of the hydrogen used in the reduction may have a deleterious effect. Thus, it has been found that reduction of a catalyst by hydrogen containing as little as 0·1 *per cent.* nitrogen results in the coverage of as much as 20 *per cent.* of the iron surface with chemisorbed nitrogen [4]. It is also known that chemisorbed hydrogen and/or nitrogen inhibits subsequent chemisorption of carbon monoxide [5].

For these reasons not too much weight should be placed on the quantitative differences as far as the percentage of chemisorbed carbon monoxide is concerned, except that it illustrates tha paramount importance of pretreatment of the surface of a catalyst. The present investigation confirms the fact that chemisorption of carbon monoxide by synthetic-ammonia-type catalysts does cocur. However, the reasoning of Emmett and his school, i.e., that carbon monoxide chemisorption is a measure of the free iron surface, becomes questionable in the light of the following observations. If carbon monoxide chemisorption occurs on iron atoms, one would naturally expect very pronounced chemisorption with pure iron surfaces. Podgurksi and Emmett[6] have found, however, that only about 10 *per cent.* of the surface of very pure iron wire, iron powder from the reduction of hematite and iron powder from iron carbonyl can be covered by chemisorbed carbon monoxide at temperatures of −195°C and −80°C.

Since magnetite is the starting material in the preparation of fused synthetic-ammonia-type catalysts, it was deemed expedient to investigate carbon monoxide chemisorption on iron particles obtained by hydrogen reduction of a pure synthetic magnetite. For this purpose some 30 g magnetite were prepared from a solution of equal amounts of ferrous and ferric iron as the analar chlorides by precipitation with ammonia to the exclusion of atmospheric oxygen[7]. The precipitate was twice washed with distilled water by decantation and filtered on a Buchner funnel. The material was partly dried at room temperature in a vacuum desiccator and subsequently heated at 200°C in oxygen-free nitrogen. X-ray examination showed it to be magnetite consisting of crystallites of the order of 500 Å with a small amount (say 5 *per cent.*) of α-Fe_2O_3. Spectrochemical analysis showed that it contained only 0·006% Cu, 0·02% Mn, 0·006% Mg and no potassium.

This sample was reduced at 450°C for 15 hours with tank hydrogen purified by passage through a "Deoxo" tube and dried by means of anhydrous magnesium perchlorate. An adsorption run with carbon monoxide at −183°C carried out in the manner described above revealed no chemisorption whatsoever. The iron powder was then heated for a further 8 hours at 450°C in specially pure hydrogen (see experimental) and once again no sign of carbon monoxide chemisorption was observed.*

This result does not imply that carbon monoxide cannot be chemisorbed on metal surfaces such as iron or other transition metals. Chemisorption has been clearly established by investigations on metal surfaces which were prepared with the utmost precaution in order to give surfaces free from any appreciable amounts of contaminants[8]. The failure to establish chemisorption with iron powder prepared from magnetite only goes to show the difficulties encountered in investigating chemisorption on bulk materials such as catalysts due to surface contamination effects. The pertinent fact that promoted catalysts exhibit certain though varying amounts of chemisorption of carbon monoxide, while pure iron, tested under similar conditions, shows no or very little chemisorption, still remains to be explained.

In conclusion it should be pointed out that the above considerations apply only to synthetic-ammonia-type catalysts. The composition and structure of precipitated catalysts are so different that the method of determination of the free iron surface is not applicable to this type of catalyst.

2. High temperature chemisorption of carbon monoxide and hydrogen.

Adsorption isobars for the adsorption of carbon monoxide on the catalysts over the range of 0°C to 300°C are shown in Figures 3 and 4. These isobars depict the

* On repeating this experiment with an adsorption apparatus in which all essential greased stop-cocks had been replaced by mercury cut-offs chemisorption of carbon monoxide was in fact found. The fraction of the total adsorption due to chemisorption was, however, only about 15%. Haul, R.A.W. and Swart, E. R. (unpublished).

variation of the amount of carbon monoxide adsorbed at constant pressure as a function of the temperature and were obtained from plots of isotherms for each catalyst at suitable temperature intervals over the range. The isobars are given for constant pressures of 150 mm and 350 mm.

Adsorption isobars often behave in the way observed with catalyst C (Figure 3) and can be satisfactorily explained in the following manner. At the lower temperatures adsorption is mainly physical adsorption and, because this process is exothermic, the amount of adsorption decreases with increase of temperature. As the temperature is raised the rate of chemisorption increases. This effect counterbalances the decrease first observed and finally results in an increase of the total amount adsorbed. When the temperature is sufficiently high, chemisorptive equilibrium is established and, since this process is also exothermic, the extent of adsorption decreases again when the temperature is increased still further.

The precipitated catalysts C and D show a minimum of carbon monoxide adsorption at 95°C to 100°C. With catalyst A the minimum shifts to approximately 80°C while, in the case of B, the value is about 115°C. With C chemisorptive equilibrium is apparently established at about 225°C and it may be significant that this temperature is the one actually employed for the synthesis of hydrocarbons with this particular catalyst. Contrary to C the other catalysts exhibit no maximum adsorption but show an increase of the amount adsorbed with increase of temperature. This observed increase can only be attributed to the onset of some chemical reaction whereby carbon monoxide is being used up. Thus, in the course of their studies at 0°C — 108°C on the adsorption of carbon monoxide on potassium carbonate promoted iron catalysts, Probst *et al.*[9] found that chemical reactions occur which produce iron pentacarbonyl and carbon dioxide. Formation of carbides on the surface of a catalyst at elevated temperatures has also been demonstrated by various investigators.[10]

Adsorption isobars for the adsorption of hydrogen on catalysts A and C at a constant pressure of 350 mm are given in Figures 5 and 6, respectively. In the case of A a decrease in the amount of hydrogen adsorbed is noted on increasing the temperature from −183°C to −50°C. This is compatible with the concept of van der Waal's adsorption as outlined above. No indication of the "type A" activated adsorption of hydrogen by iron catalysts at −100°C as reported by Emmett and Harkness[2] was encountered. This type of low temperature activated adsorption is very sensitive to surface contamination, however, and this factor might well account for the absence of "type A" adsorption in our observations.

Chemisorption of hydrogen by both catalysts, though slight, becomes apparent from about 20°C onwards, reaching equilibrium in the region of 200°C. Chemisorption of hydrogen by catalyst C seems to be markedly temperature dependent and a sharply defined maximum is evident.

It is interesting to compare the nitrogen monolayer capacity, V_m, with the amounts of carbon monoxide and hydrogen chemisorbed at high temperatures. For this purpose a pressure of 350 mm and a temperature of 200°C, where maximum hydrogen adsorption occurs, is selected. The relevant amounts are listed in Table IV. Chemisorption of hydrogen at 200°C was not measured in the case of catalysts B and D.

Although low temperature chemisorption of carbon monoxide by the fused catalysts is relatively small, obviously as a result of surface contamination, the amounts chemisorbed at 200°C compare favourably with the nitrogen monolayer capacities. The amounts of carbon monoxide chemisorbed by the precipitated catalysts, on the other hand, are only fractions of the respective monolayer capacities. This is in accordance with the low temperature measurements where chemisorption of carbon monoxide by these catalysts is also negligibly small.

TABLE IV

Comparison of nitrogen monolayer capacities with amounts of chemisorbed carbon monoxide and hydrogen.

Catalyst	$V_m(N_2)$ cc N.T.P./g	V_{CO} chemisorbed at −183°C cc N.T.P./g	V_{CO} chemisorbed 350 mm, 200°C cc N.T.P./g	V_{H_2} chemisorbed 350 mm, 200°C cc N.T.P./g
A	1·61	0·24	1·5	0·67
B	1·50	0·22	1·45	—
C	47·0	—	1·25	25
D	39·5	1·0	1·40	—

Rather surprisingly the precipitated catalyst C exhibits pronounced hydrogen chemisorption at 200°C. This must be attributed to the chemisorption of hydrogen by the oxides which are present in the catalyst as carriers and/or promoters. High temperature chemisorption of hydrogen on various oxides is well known, e.g. in the catalytic synthesis of methanol hydrogen is chemisorbed on a zinc oxide catalyst. Schuster[11] has investigated the adsorption of hydrogen on catalyst carriers.

Despite the fact that studies of the chemisorption of carbon monoxide and hydrogen in the temperature range of the synthesis are of direct interest in connection with possible reaction mechanisms, only a few such investigations have been published so far. Matsumura *et al.*[12], working with cobalt and iron catalysts, have observed that hydrogen exhibits an adsorption maximum at about 200°C while carbon monoxide adsorption increases steadily with temperature. This is in agreement with our observations in the present study. Recently, Ghosh *et al.*[13] have investigated adsorption on cobalt catalysts from mixtures of carbon monoxide and hydrogen. The temperature range in these experiments was limited, however, since reaction occurred between the components above 100°C. Nevertheless, these studies established that the larger the amount and rate of chemisorption of either carbon monoxide or hydrogen, the greater the activity of the catalysts, i.e., the percentage conversion and yield of hydrocarbons.

3. Rates of chemisorption of carbon monoxide.

The kinetics of the chemisorption of carbon monoxide by catalysts C and D were investigated over the temperature range 140°C — 180°C. This range was chosen because the rates were conveniently measurable and the temperature sufficiently low to ensure that the rate of desorption was negligible.

For a quantitative interpretation of adsorption rate measurements it is desirable to measure the rates at constant pressure. The design of our present apparatus did not permit this, however, and a correction had to be applied to compensate for the drop in pressure during the course of the measurements. The rates actually determined by graphical differentiation of the adsorption versus time curves were, therefore, corrected to the mean pressure of the experiment. This was done on the basis that the rate, at a given temperature and for a given amount of adsorption, varies linearly with pressure as has been found by Ghosh *et al.*[13].

Taylor[14], who originated the concept of activated adsorption, proposed the following rate equation:

$z = ap(1-\theta)e^{-E_A/RT}$ where z = adsorption rate, θ = coverage, p = pressure, a = a constant and E_A = energy of activation of the adsorption process.

In this equation the rate of desorption is taken as neglibigle.

If we assume this equation to be valid for the adsorption of carbon monoxide on catalysts C and D, respectively, the activation energy can be calculated in each case from the change of the rate of adsorption with temperature at constant coverage:

$$E_A = 2{\cdot}303\ R\ (\log z_1 - \log z_2)/\ \frac{1}{T_1} - \frac{1}{T_2}$$

From the plot of E_A against amount adsorbed (Figure 7), it is evident that, for each catalyst, the activation energy for the adsorption of carbon monoxide exhibits a small linear dependence on coverage. Since this effect is not pronounced no great error is introduced in any subsequent calculation by taking E_A as constant at 15,000 and 14,700 calories for catalysts C and D respectively.

From the Taylor equation we have:

$$ap\ (1-\theta) = z{\cdot}e^{E_A/RT}$$

The temperature independent term $ap\ (1-\theta)$ can now be evaluated since the rate of adsorption z as well as the activation energy E_A are known as functions of the amount of carbon monoxide adsorbed. It was found that the value of $ap\ (1-\theta)$ decreases markedly with coverage. When plotted on a semi-logarithmic scale, linear plots were obtained for both catalysts, thereby indicating that the temperature independent term is an exponential function of the coverage in each case. One such plot is depicted in Figure 8.

A combination of all results shows that the rate of adsorption of carbon monoxide by catalysts C and D over the occupation range 0·15 — 0·50 cc N.T.P./g and for a pressure of 250 mm Hg may be represented by:

$z = 5{\cdot}66{\cdot}10^{10}{\cdot}e^{(-5{\cdot}13V)}e^{(-15,000/RT)}$ sec^{-1} for catalyst C,

and

$z = 3{\cdot}18{\cdot}10^{10}{\cdot}e^{(-5{\cdot}04V)}e^{(-14,700/RT)}$ sec^{-1} for catalyst D,

where

V = cc N.T.P./g.

For conditions of constant temperature each of the above equations reduces to an equation of the form

$z = c{\cdot}e^{-gV}$, where c and g are constants.

This is identical with the Zeldowitch[15] equation which has been applied with success to a number of adsorption processes.

As in the case of high temperature adsorption measurements, surprisingly few studies on the rates of chemisorption on F.T. catalysts have been reported. Following investigations by Emmett and Brunauer[16] and Brunauer, Love and Keenan[17] a study of the kinetics of the chemisorption of nitrogen on synthetic-ammonia-type catalysts has been reported by Zwietering and Roukens[18]. A feature of this work is the exactitude with which the experimental procedure has been carried out. The main result is that the activation energy for the chemisorption of nitrogen on singly promoted iron catalysts is a linear function of the coverage up to about $\theta = 0{\cdot}25$. The activation energy changes from 8 — 30 k.cal/mole whereafter it seems to remain constant. Unfortunately no rates were measured at $\theta > 0{\cdot}3$.

In the analysis of their results the authors apply the Taylor equation and the temperature independent factor of the rate equation was evaluated against coverage in the same way as in the present study (see Figure 8). We should expect to find a curve depreciating with increasing θ on which all the data measured at the different

temperatures should correlate. This is, in fact, the case in the present study. In the work of Zwietering and Roukens the curve, instead of falling, showed an increase with θ. The authors consequently assume that a decrease of the rate of adsorption due to an increase of activation energy is compensated for by a change of the temperature independent term of the rate equation. As an explanation they suggest either a change-over from the immobile to the mobile state of adsorption, or a temperature dependency of the activation energy.

It must be pointed out, however, that the original Taylor equation is based on the assumption of a constant activation energy. This assumption is fairly justified in the present experiments. In the nitrogen chemisorption measurements, however, the activation energy changes more than twofold in the range of coverage studied and the original Taylor equation can no longer be expected to be valid. In its stead a rate equation derived by Brunauer *et al.*[17] from the Taylor equation by assuming a linear increase of activation energy with suface coverage should be used. An attempt to present the data of Zwietering and Roukens in this way met with no success and the indications are that fundamental shortcomings exist in the theory of the kinetics of chemisorption.

The kinetics of the chemisorption of carbon monxoide and hydrogen on cobalt F.T. catalysts has been studied by Ghosh *et al.* at a few temperatures in the range 150°C — 200°C. From an empirical equation the authors derived apparent activation energies and found that the activation energies increase with the amount adsorbed and decrease with increasing pressure. Thus, activation energies of 6 — 20 k.cal/mole were observed depending on the experimental conditions. The strong dependence of the activation energy on pressure suggests that the process of adsorption is a complex one involving, not only adsorption, but diffusion within the pore system of the catalyst as well. In this work no attempt was made to differentiate between the adsorption proper and transport processes.

CONCLUSIONS

1. Low temperature chemisorption of carbon monoxide and carbon dioxide on some precipitated and synthetic-ammonia-type catalysts were studied in order to determine the relevant fractions of the surfaces occupied by iron and potassium oxide and/or aluminium oxide, respectively. In agreement with Emmett and his school chemisorption was observed in some cases although to a lesser extent, which is attributed to incomplete removal of contaminants from the surfaces of the catalysts. Pure iron powder obtained by the reduction of pure synthetic magnetite exhibited no chemisorption of carbon monoxide. Since Emmett *et al.* also found only very little chemisorption on pure iron, the difference in behaviour of pure iron and promoted iron needs to be explained.

2. High temperature chemisorption of carbon monoxide showed chemisorptive equilibrium, i.e., a maximum in the adsorption isobar only in the case of the precipitated catalyst C. With the other precipitated catalyst as well as the fused catalysts, chemisorption increases steadily with a rise in temperature. This must be attributed to the onset of some chemical reaction. Isobars for the chemisorption of hydrogen on catalysts A and C show a maximum at about 200°C in each case. The amount of hydrogen adsorbed in comparison with the amount of carbon monoxide, in the case of the precipitated catalyst, suggests that the hydrogen is adsorbed by the oxides present in the catalyst as carriers and/or promoters.

3. Rates of chemisorption of carbon monoxide on the precipitated catalysts C and D were measured over the temperature range 140°C — 180°C. From the measurements an apparent activation energy of 15 k.cal/mole was found for both catalysts. It is shown that the Taylor adsorption equation can be applied with success.

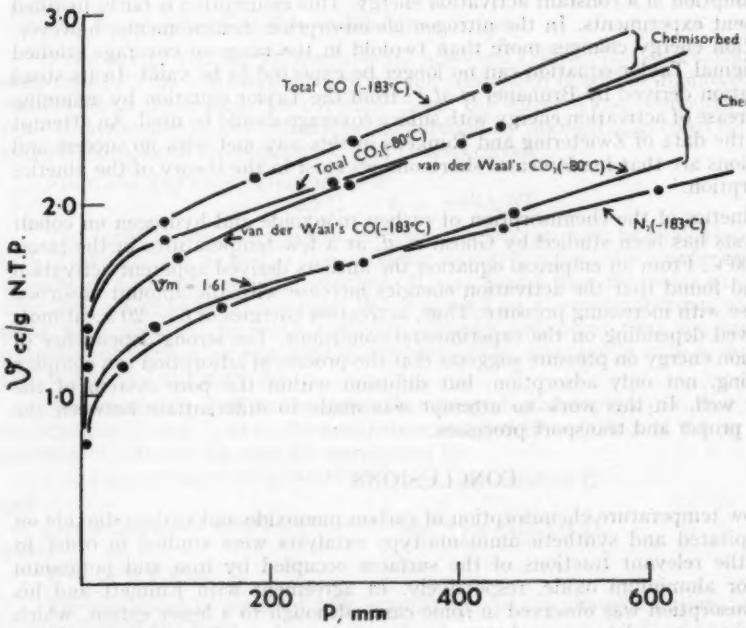

Fig. 1. Adsorption of nitrogen, carbon monoxide and carbon dioxide by catalyst A.

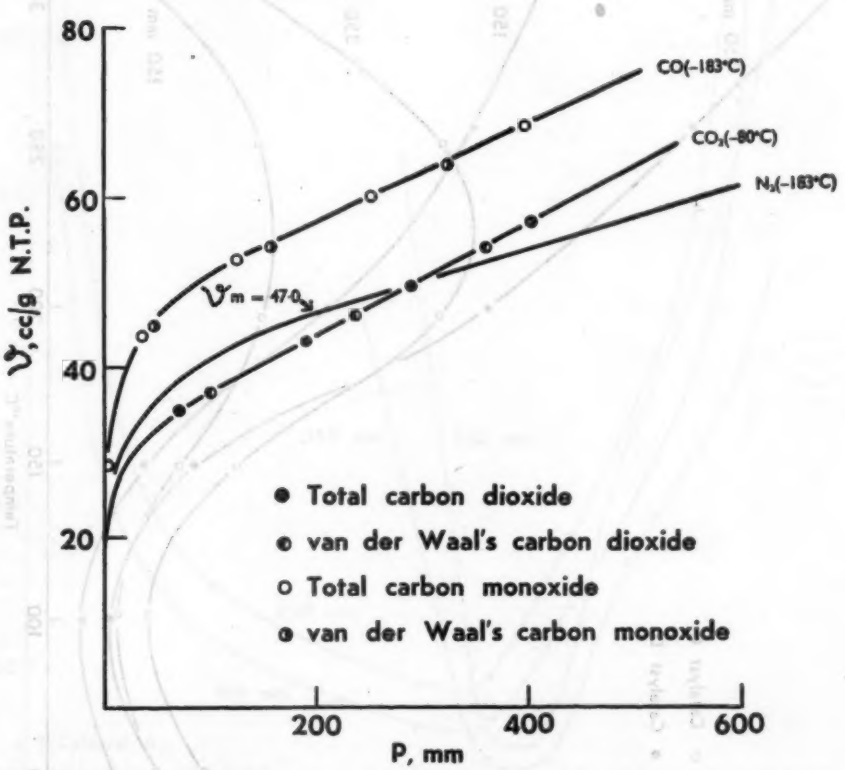

Fig. 2. Adsorption of nitrogen, carbon monoxide and carbon dioxide by catalyst C.

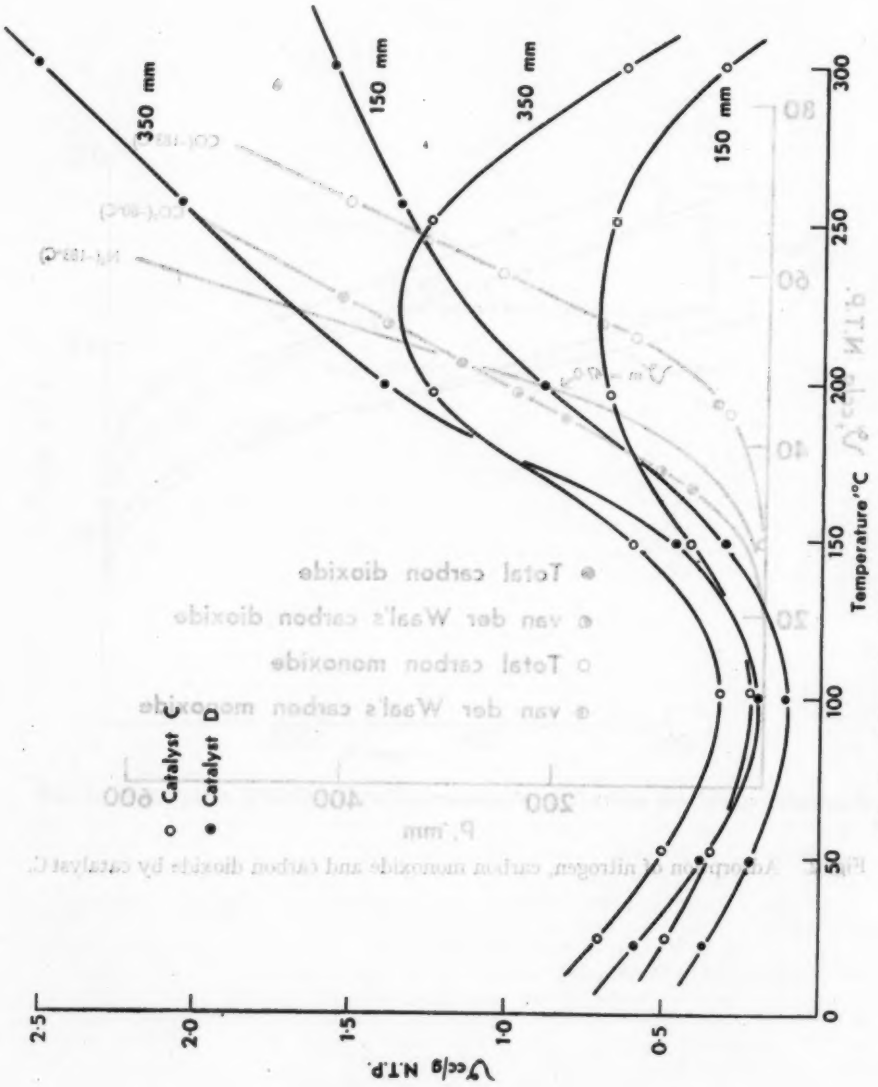

Fig. 3. Adsorption isobars of CO on catalysts C and D.

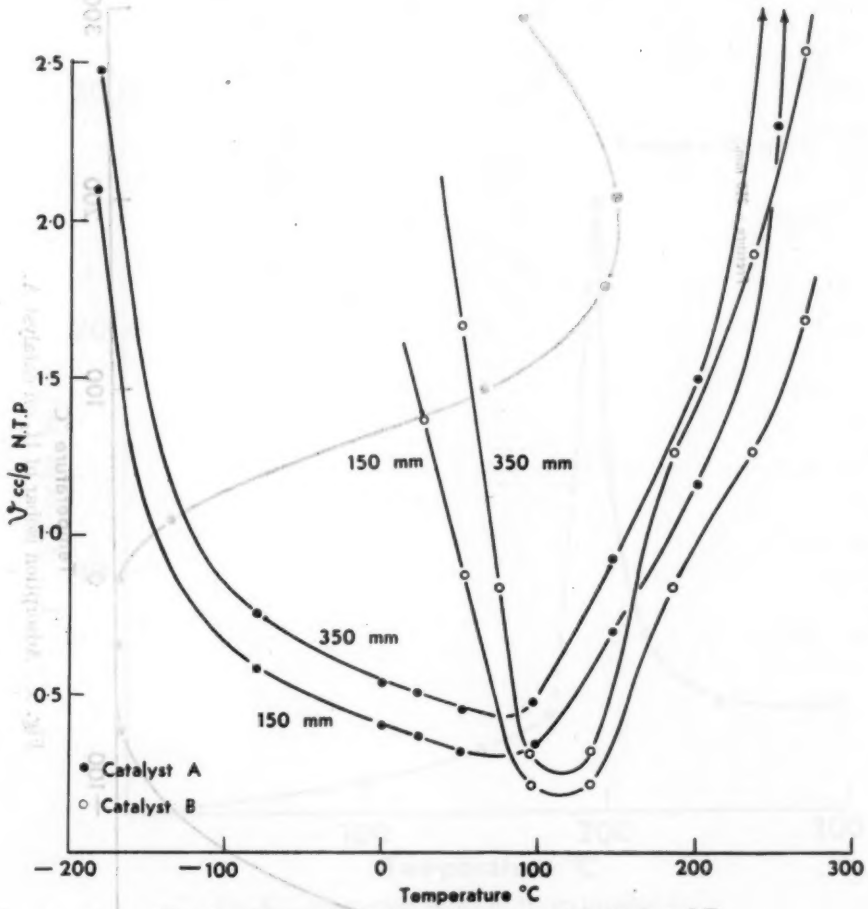

Fig. 4. Adsorption isobars of CO on catalysts A and B.

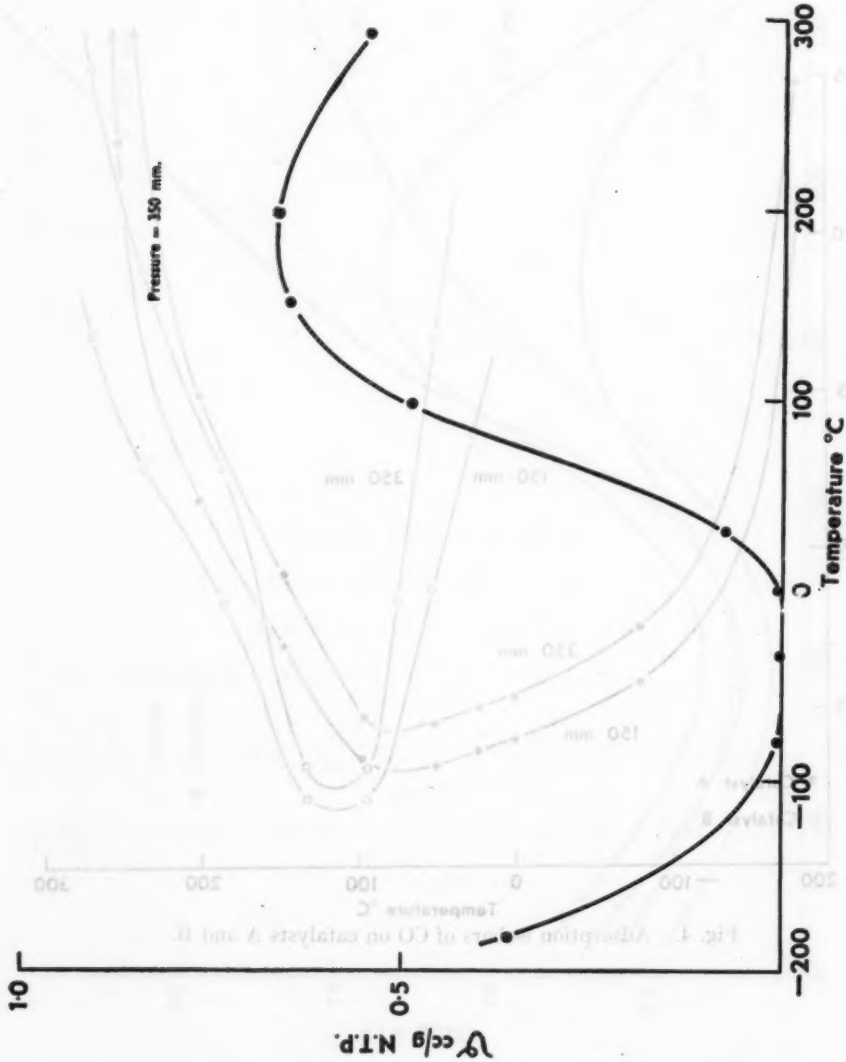

Fig. 5. Adsorption isobar of H_2 on catalyst A.

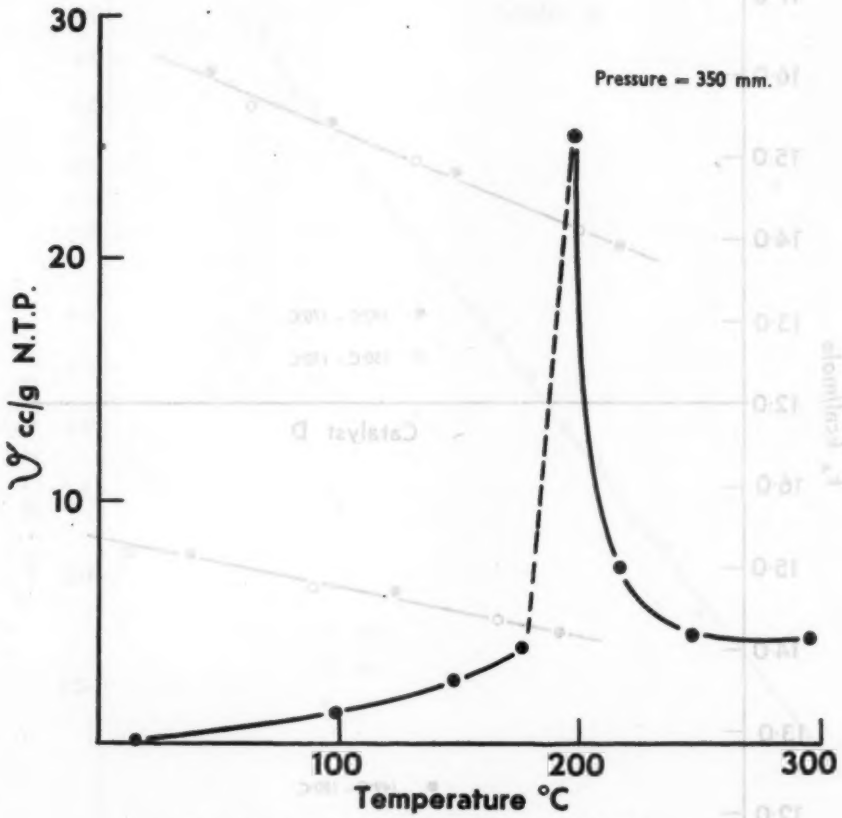

Fig. 6. Adsorption isobar of H_2 on catalyst C.

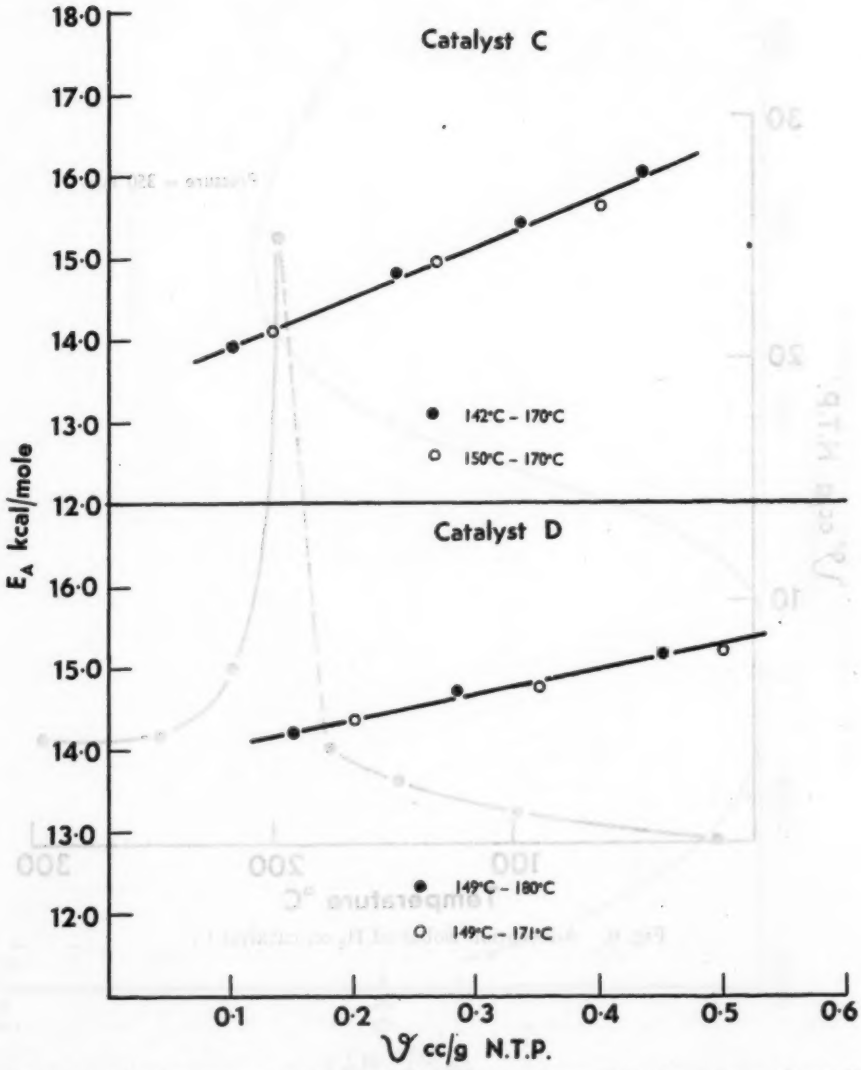

Fig. 7. Activation energy of the adsorption of carbon monoxide by catalyst C and D.

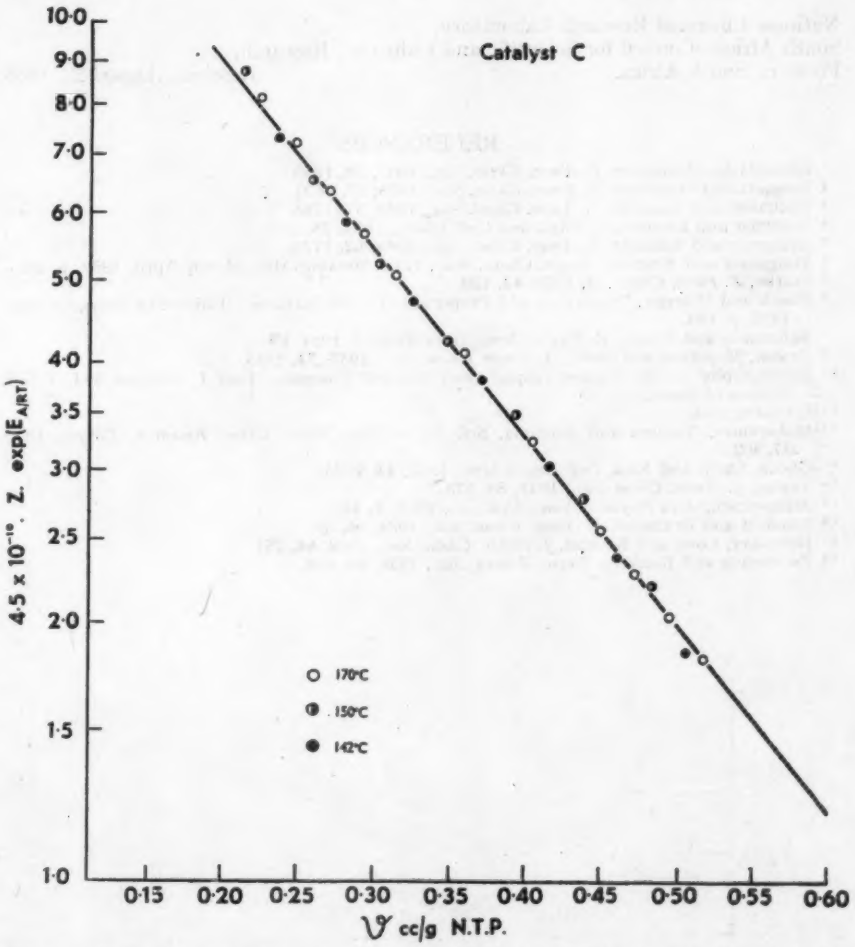

Fig. 8. Plot of the temperature—independent factor of the rate equation against v.

ACKNOWLEDGEMENTS

The author wishes to express his indebtedness to Dr. R. A. W. Haul for his interest and helpful advice.

This paper is published by permission of the South African Council for Scientific and Industrial Research.

National Chemical Research Laboratory,
South African Council for Scientific and Industrial Research,
Pretoria, South Africa. *Received, August* 22, 1955.

REFERENCES

[1] Emmett and Brunauer, *J. Amer. Chem. Soc.*, 1937, **59**, 1553.
[2] Emmett and Harkness, *J. Amer. Chem. Soc.*, 1935, **57**, 1631.
[3] Brunauer and Emmett, *J. Amer. Chem. Soc.*, 1935, **57**, 1754.
[4] Kummer and Emmett, *J. Phys. and Coll. Chem.*, 1951, **55**, 337.
[5] Brunauer and Emmett, *J. Amer. Chem. Soc.*, 1940, **62**, 1732.
[6] Podgurski and Emmett, Amer. Chem. Soc., 121st Meeting Abs., March–April, 1952, p. 29.
[7] Starke, *Z. Phys. Chem., B*, 1939, **42**, 159.
[8] Beeck and Wheeler, "Structure and Properties of Solid Surfaces", University Press, Chicago, 1933, p. 450.
Suhrmann and Schulz, *Z. Phys. Chem.*, Neue Folge I, 1954, **69**.
[9] Probst, Meyerson and Seelig, *J. Amer. Chem. Soc.*, 1952, **74**, 2115.
[10] Bibliography of the Fischer-Tropsch and Related Processes, Part I. Bulletin 544, U.S.A. Bureau of Mines.
[11] Schuster, *ibid.*
[12] Matsumura, Tarama and Kodama, *Sci. Papers Inst. Phys. Chem. Research (Tokyo)*, 1940, **37**, 302.
[13] Ghosh, Sastri and Kini, *Ind. Eng. Chem.*, 1952, **44**, 2463.
[14] Taylor, *J. Amer. Chem. Soc.*, 1931, **53**, 578.
[15] Zeldowitsch, *Acta Physiocochim., U.R.S.S.*, 1934, **1**, 449.
[16] Emmett and Brunauer, *J. Amer. Chem. Soc.*, 1934, **56**, 35.
[17] Brunauer, Love and Keenan, *J. Amer. Chem. Soc.*, 1942, **64**, 751.
[18] Zwietering and Roukens, *Trans. Farad. Soc.*, 1954, **50**, 178.

OFFICE BEARERS AND COUNCIL—1955-1956—AMPSDRAERS EN RAAD

President:

F. W. Hayes, F.R.I.C., A.M.I.Chem.E.

Immediate Past President/Vorige-president:

S. S. Israelstam, M.Sc., Ph.D., F.R.I.C.

Vice President/Vise-president:

F. Hawke, M.Sc.(Eng.), Ph.D., F.R.I.C., A.M.I.Chem.E.

Hon. Secretary and Treasurer/Ere-sekretaris en Tesourier:

M. Mrost, M.Sc., A.R.I.C.

Chairman of the Publications Committee and Librarian/Voorsitter van die Publikasies-komitee en Bibliotekaris:

S. S. Israelstam, M.Sc., Ph.D., F.R.I.C.

Members of Council/Raadslede:
S. Transvaal Section/Seksie:

F. L. Clark, M.Sc.;
G. A. Sutton Clark, B.Sc., A.R.T.C., A.R.I.C.;
S. Goodman, B.Sc.(Eng.);
G. S. James, O.B.E., B.Sc.(Hons.);
H. A. E. Mackenzie, M.Sc., Ph.D., D.I.C., A.R.I.C.

Natal Section/Seksie:

W. A. Dark, B.Sc., Ph.D., D.I.C., A.R.I.C., A.M.I.Chem.E.;
H. N. C. MacLennan, B.Sc.(Eng.), A.R.I.C., A.M.I.Chem.E.;
A. F. Strangman, M.Sc.

Pretoria Section/Seksie:

G. W. Perold, D.Sc., D.Sc.Tech.;
C. C. van der Merwe, M.Sc.;
J. van Garderen, D.Sc., F.R.I.C.

E. Province/O. Provinsie Seksie:

R. Paget, B.Sc., A.R.I.C.;
R. Schauder, B.Sc.

W. Province Section/W. Provinsie Seksie:

A. Antonis, B.Sc., Ph.D.;
E. N. Costa, B.Sc.;
Prof. E. F. C. H. Rohwer, M.Sc., Dr. rer. Nat.

VIR DIE AANDAG VAN OUTEURS

Die Joernaal van die Suid-Afrikaanse Chemiese Instituut word gewy aan die publikasie van oorspronklike navorsing in alle vertakkings van chemie en chemiese tegnologie.

Alle bydraes moet in triplikaat ingehandig word; indien daar grafieke is moet een stel noukeurig met *Oosindiese ink afgeteken word op gladde wit Bristol-blad of tekenpapier, of op aftrekdoek* —die ander twee stelle kan afdrukke wees, of met potlood geteken word.

Artikels moet so saaklik moontlik wees, verenigbaar met duidelikheid, en moet nie onnodige eksperimentele besonderhede bevat nie. Artikels moet *in tikskrif wees—dubbel spasiëring*—net aan een kant van die papier, met 'n behoorlike kantruimte aan die linkerkant. Die papier moet nie-absorberend wees.

Die buitemate van plate—insluitende die ruimte vir byskrif—moet hoogstens 14 duim by 10 duim wees, en liefs nie minder as 7 duim by 5 duim nie. Die verhouding 1·4:1·0 moet in elk geval nagekom word. Byskrif en letters—hetsy in die kantruimte of in die tekening self—moet nie met ink gedoen word nie, *maar liggies met gewone potlood of uitveebare bloupotlood.*

Elke artikel moet voorafgegaan word deur 'n opsomming in elk van die twee offisiële landstale, en die opsomming wat tweede verskyn moet in dieselfde taal as die artikel wees. Die opsomming moet in eenvoudige taal 'n kort en saaklike uiteensetting gee van die oogmerke van die ondersoek, die resultate wat behaal is, en die gevolgtrekkings. Die opsomming moet ongeveer 50-250 woorde beslaan en mag in elk geval nie meer as 5 persent van die artikel wees nie.

Verwysings moet in numeriese opeenvolging aan die end verskyn, in die volgorde: skrywer se van; skrywer se voorletters; joernaal; datum; deel; bladsy; die ooreenstemmende verwysingsnommers moet in volgorde in die teks verskyn as kopskrifte.

Verwysings na boeke moet as volg aangedui word: skrywer se van; skrywer se voorletters; titel; uitgawe; uitgewer; datum van publikasie; bladsy.

Simbole en afkortings moet volgens B.S. 813: 1938 wees.

Bydraers moet afskrifte hou van al hulle mededelings.

Outeurs word versoek om hulle bydraes so op te stel dat dit ooreenstem met die gewone trant konvensie en hernagtigheid van hierdie joernaal.

Dui asseblief aan waarheen die drukproewe moet gestuur word.

Outeurs kan verdere voorskrifte en aanwysings, i.v.m. die opstel van 'n artikel, aanvra.

Rig asseblief alle korrespondensie aan die Redakteur van die Joernaal, Suid-Afrikaanse Chemiese Instituut, Kelvinhuis, h/v Marshall- en Hollardstraat, Johannesburg.

NOTICE TO AUTHORS

The Journal of the South African Chemical Institute is designed for the publication of origina work in all branches of chemistry and chemical technology.

All papers must be submitted in triplicate: where diagrams are included one set of these must be carefully drawn, *in Indian ink, on smooth white Bristol board or paper, or on tracing cloth*, the remaining two copies may be pencil drawings or prints.

Papers should be as brief as possible compatible with clarity, and no unnecessary experimental details should be included. All papers must be *typewritten in double line spacing*, on one side only of the paper, with a good margin on the left hand side. The paper should be non-absorbent.

The total external dimensions of illustrations (including space to be taken up by lettering) should not exceed 14 inches by 10 inches and preferably should not be less than 7 inches by 5 inches—the proportion 1·4:1·0 being in all cases maintained. Lettering on drawings, whether on the margin or in the body of the drawing must not be in ink but must be inserted *lightly, in blue pencil or erasable lead pencil.*

Every paper must be preceded by two summaries, one in each official language; the second summary being in the same language as that of the paper. Each summary should set forth concisely and in simple language the objects and purpose of the investigation, the results obtained and conclusions drawn. These should normally be from 50 to 250 words in length and, in any case, should not exceed 5 per cent. of the paper.

References should appear at the end of the paper, in numerical order in the following sequence: author's surname; author's initials; journal; date; volume number; page; the necessary reference numbers should appear, in sequence, as superscripts in the text.

Where reference is made to books the following sequence should be adhered to: author's surname; author's initials; title; edition; publisher; date of publication; page.

Symbols and abbreviations used should conform with B.S. 813: 1938.

Authors should retain copies of their communications.

Authors are requested to arrange their papers to conform, as far as possible, with the normal style, conventions and concisenss of this journal.

The address to which proofs are to be sent should be written on every paper.

Directions to authors regarding the preparation of papers will be forwarded on application.

All communications should be addressed to the Editor of the Journal The South African Chemical Institute, Kelvin House, cor. Marshal and Hollard Streets, Johannesburg.

C.P.W.—P.M.B. 5